

Deciphering Functions of Neurons in Vision-Language Models

Jiaqi Xu*
 xujaqi@mail.ustc.edu.cn
 University of Science and Technology
 of China
 Hefei, Anhui, China

Cuiling Lan
 culan@microsoft.com
 Microsoft Research Asia
 Beijing, China

Yan Lu
 yanlu@microsoft.com
 Microsoft Research Asia
 Beijing, China

Abstract

The burgeoning growth of open-source vision-language models (VLMs) has catalyzed a plethora of applications across diverse domains. Ensuring the transparency and interpretability of these models is critical for fostering trustworthy and responsible AI systems. In this study, our objective is to delve into the internals of VLMs to interpret the functions of individual neurons. We observe the activations of neurons with respects to the input visual tokens and text tokens, and reveal some interesting findings. Particularly, we found that there are neurons responsible for only visual or text information, or both, respectively, which we refer to them as visual neurons, text neurons, and multi-modal neurons, respectively. We build a framework that automates the explanation of neurons with the assistance of GPT-4o. Meanwhile, for visual neurons, we propose an activation simulator to assess the reliability of the explanations for visual neurons. System statistical analyses on top of one representative VLM of LLaVA, uncover the behaviors/characteristics of different categories of neurons.

CCS Concepts

• Computing methodologies → Artificial intelligence.

Keywords

VLMs; neuron function; activations; interpretability

ACM Reference Format:

Jiaqi Xu, Cuiling Lan, and Yan Lu. 2025. Deciphering Functions of Neurons in Vision-Language Models. In *Proceedings of the 33rd ACM International Conference on Multimedia (MM '25), October 27–31, 2025, Dublin, Ireland*. ACM, New York, NY, USA, 24 pages. <https://doi.org/10.1145/3746027.3755003>

1 Introduction

The advent of vision-language models (VLMs) has ushered in a new era in the field of artificial intelligence, where the synergy between visual perception and language understanding has been leveraged to solve complex tasks, such as image captioning, visual question answering, and multi-modal information retrieval. They have found widespread application across various domains, including, but not limited to, embodied AI, agents, and human-machine interaction.

*This work was done when Jiaqi was an intern at Microsoft Research Asia. This paper is the result of an open source research project.



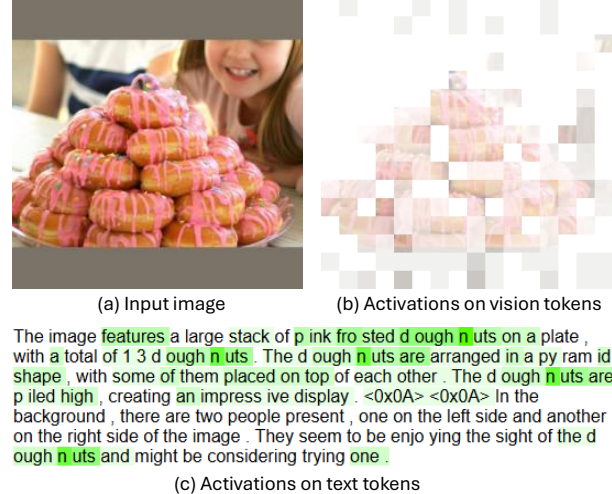
This work is licensed under a Creative Commons Attribution-ShareAlike 4.0 International License.

MM '25, Dublin, Ireland

© 2025 Copyright held by the owner/author(s).

ACM ISBN 979-8-4007-2035-2/2025/10

<https://doi.org/10.1145/3746027.3755003>



The image features a large stack of pink frosted doughnuts on a plate, with a total of 13 doughnuts. The doughnuts are arranged in a pyramid shape, with some of them placed on top of each other. The doughnuts are piled high, creating an impressive display. <0x0A> <0x0A> In the background, there are two people present, one on the left side and another on the right side of the image. They seem to be enjoying the sight of the doughnuts and might be considering trying one.

Figure 1: To understand the function of a neuron, we observe the activations of this neuron on visual tokens and text tokens for each sample. To facilitate visualization, for visual tokens, a higher transparent degree indicates a higher activation; for text tokens, the darker of the green color indicates a higher activation.

The proliferation of open-source VLMs, such as LLaVA [17], BLIP-2 [13], QwenVL [1], PaliGemma [6], InternVL 2.5 [9], and others, has significantly democratized access to cutting-edge AI technologies, facilitating researchers and practitioners to build upon these foundations to create innovative applications that span educational, medical, and entertainment spheres. However, the complexity and opacity of these models often pose a significant challenge to their broader adoption, particularly in domains where trustworthiness, transparency, and accountability are paramount. The black box nature of VLMs, has raised concerns regarding the interpretability of these models. Bills *et al.* [7] investigated the automatic explanation of neurons in Language Model with pure texts as input. Understanding the internal workings of VLMs, including the functions of neurons and how they treat vision and text differently, is crucial for ensuring that these systems operate in a manner that is interpretable to human users.

In this paper, we aim to shed light on the internal mechanisms of VLMs by exploring the functions of individual neurons within a VLM. Specifically, we seek to understand whether neurons within VLMs exhibit different responses to visual and text tokens, and whether there exist specialized neurons dedicated to processing visual-specific or text-specific information. How are such neurons distributed across the network? How can we automatically interpret

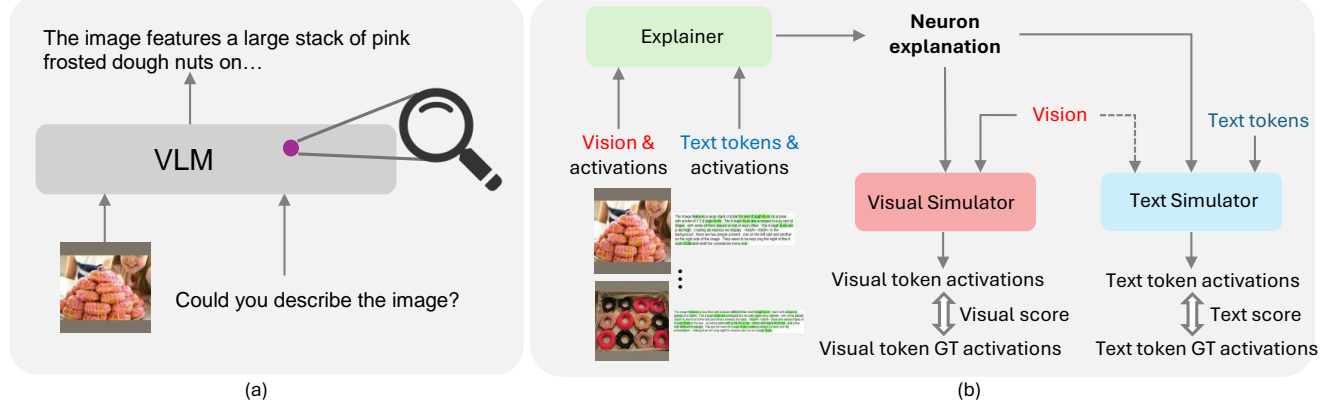


Figure 2: Illustration of our main workflow for investigating neuron functions in a VLM (e.g., LLaVA). (a) A VLM takes an image and a text prompt as input, and output the predicted texts. For each neuron, we obtain its activations with respect to each visual token and text token in an input sample (see Figure 1). We record the activations for the top N samples with the highest activation values (which we refer to as top-activated samples) of the dataset for further analysis. (b) For each neuron, based on the top-activated samples and their activations, the explainer automatically generates an explanation of the neuron function. The visual simulator and text simulator estimate the activations for the visual and text tokens, respectively, based on the explanation. We evaluate the reliability of each explanation by computing the correlation between the simulated activations and the actual (i.e., ground-truth) activations.

the functions of neurons and assess the reliability of the explanation? Are there neurons that possess functions that provide insights comprehensible to humans?

To achieve our objectives of unveiling the mystery of VLMs, we systematically observed the responses of neurons with respect to visual tokens and text tokens, where Figure 1 shows an example of the visualization of neuron responses for visual and text tokens. Through extensive observations of diverse neuronal response patterns, we have uncovered several interesting findings, including the existence of visual-specific neurons, text-specific neurons, and multi-modal neurons. These discoveries provide a broad overview of neuron functions and enable our statistical analyses of neuron distribution. In addition, as illustrated in Figure 2 (b), to enable automated interpretation of neuron functions, we introduce a framework that leverages GPT-4o as an explainer to generate functional interpretations of individual neurons. We also develop two simulators: a visual simulator for evaluating the robustness of explanations targeting vision-related neurons, and a text simulator for evaluating the robustness of explanations targeting text-related neurons. Moreover, we conducted statistical analyses on a representative VLM, LLaVA-1.5 [17], uncovering the behaviors/characteristics of different neuron categories. Similar observations were found in other typical VLMs, such as InternVL 2.5 [9] and Qwen2.5-VL [3] (see Section 8 and Section 9 in the Supplementary).

In summary, we have four main contributions:

- We analyze the internal mechanisms of VLMs to interpret the functions of neurons. Based on the activation patterns in response to visual and text tokens, we reveal the existence of neurons that are responsible for only visual or text information, as well as neurons that respond to both modalities.
- We systematically observe neuron activations and provide a broad overview of their functional roles. A mechanism is introduced to identify vision-, text-, and multi-modal neurons.

- We introduce a framework that enables the automatic interpretation of VLM neuron functions, along with an activation simulator to predict token activations and facilitate the evaluate of explanation reliability.
- We conducted extensive analyses of the characteristics of different neuron categories to enable a more comprehensive understanding. Our findings include, for example, multi-modal neurons tend to appear more frequently in higher layers, while other neurons are more common in low layers; pruning of certain unknown neurons results in only marginal performance degradation; there are outlier neurons that are strongly activated for most tokens across all samples.

We hope that our work inspires further research to advance the development of transparent, trustworthy, and responsible AI systems.

2 Related Work

Vision-Language Models (VLMs) VLMs are designed to process and understand both visual and textual data simultaneously. Recent advancements, such as those presented by LLaVA [17], BLIP-2 [13], Qwen-VL [1], and PaliGemma [6], demonstrate the rapid evolution and expanding capabilities of these models. A representative model, LLaVA, aligns the visual tokens (that are encoded by CLIP encoder) with the text space as input to a Large Language Model (LLM), enabling visual understanding capability [15, 17]. These systems have been instrumental in pushing the boundaries of what is possible in tasks such as image captioning, visual question answering, and multi-modal information retrieval. Our work builds on these foundations and focuses on the interpretability of VLMs – an essential aspect for their broader adoption and trustworthiness.

Interpretability in AI The interpretability of AI systems has garnered significant attention, driven by the need for transparency,

Visual neuron: layer:27, neuron:3900
Max visual activation:8, max text activation:0



The image features a large jet airplane parked together on a runway. The motor cycles are arranged in various positions, with some closer to the airplane and others further away. There are at least 13 motor cycles visible in the scene, with some located near the center, others on the left side, and a few on the right side of the image. <0x0A> <0x0A> In addition to the motor cycles, there are several other objects in the scene, including a car and a truck, and the other closer to the center. The jet airplane is prominently displayed in the background, occupying a significant portion of the image from the top left to the bottom right. The combination of the motor cycles and the airplane creates an interesting and unique scene.

(a)

Multi-modal neuron: layer:31, neuron:1800
Max visual activation:5, max text activation:9



The image features a large stack of pink frosted doughnuts on a plate, with a total of 13 doughnuts. The doughnuts are arranged in a pyramid shape, with some of them placed on top of each other. The doughnuts are piled high, creating an impressive display. <0x0A> <0x0A> In the background, there are some other items on the left side and another on the right side of the image. They seem to be enjoying the sight of the doughnuts and might be considering trying one.

(d)

Text neuron: layer:2, neuron:4450
Max visual activation:0, max text activation:10



The image features a room filled with a large collection of stuff and clutter. There are several hot dogs displayed in various positions, with some sitting on chairs and others placed on the floor. The room appears to be a store or a display area for these stuff and clutter. <0x0A> <0x0A> There are several chairs in the room, with one located near the left side, another in the middle, and a third one on the right side. A book can be seen placed on the floor, close to the left side of the room. The room is filled with a variety of stuff and clutter, creating a lively and inviting atmosphere.

(b)

Multi-modal neuron: layer:21, neuron:6100
Max visual activation:5, max text activation:10



The image features a man standing in a kitchen, holding up his thumb in a thumbs-up gesture. He appears to be cooking food on a grill, with several hot dogs visible on the grill. The man is wearing a tie, which suggests that he might be dressed up for a special occasion or event. <0x0A> <0x0A> The kitchen is well-equipped with a dining table and several chairs placed around it. There are also a few bowls and a spoon on the table, possibly containing red lentils or beans for the meal being prepared.

(c)

Multi-modal neuron: layer:29, neuron:600
Max visual activation:10, max text activation:4



The image features a man standing in a kitchen, holding up his thumb in a thumbs-up gesture. He appears to be cooking food on a grill, with several hot dogs visible on the grill. The man is wearing a tie, which suggests that he might be dressed up for a special occasion or event. <0x0A> <0x0A> The kitchen is well-equipped with a dining table and several chairs placed around it. There are also a few bowls and a spoon on the table, possibly containing red lentils or beans for the meal being prepared.

Multi-modal neuron: layer:21, neuron:6100
Max visual activation:5, max text activation:9



The image depicts a city street scene with a white fire hydrant prominently placed on the sidewalk. A group of pigeons is gathered around the fire hydrant, drinking water from it. There are at least 12 birds visible in the scene, with some standing closer to the hydrant and others further in the background. The fire hydrant is scattered throughout the field. <0x0A> <0x0A> In addition to the birds and the fire hydrant, there are several people walking along the sidewalk, with a total of 11 people visible in the image. Some of them are carrying handbags, with three having bags in the scene. <0x0A> <0x0A> The scene is also busy with traffic, as there are two cars and a truck visible in the background, indicating a bustling urban environment.

(f)

Figure 3: Visualization of neuron function categories. The caption above each sub-figure specifies the neuron category (visual, text, or multi-modal neuron), neuron id, and the max activation values for visual and text tokens, normalized on a scale from 0 to 10. Positioned centrally to the left within each sub-figure is the original image, whereas the image to the central right showcases the visualization generated post-activation by the authentic activation values of the corresponding image patches. Beneath each sub-figure, the text tokens alongside their respective activations are displayed. The darker the green, the greater the activation value.

accountability, and trust in AI applications [5, 7, 19, 24, 27, 30]. The black-box nature of many sophisticated AI models, including VLMs, poses challenges to understanding their decision-making processes. Bills *et al.* [7] explore automatic explanation mechanisms for language models, but the interpretability of VLMs remains largely unexplored.

Several works have proposed methods to explain neurons in visual models [2, 4, 8, 11, 12, 20, 21, 26]. Network Dissection [4] quantifies the interpretability of CNN by aligning the activation patterns of a neuron with predefined semantic concepts. MILAN [12] generates descriptions by searching for natural language strings that maximize mutual information with neuron activation regions. MAIA [26] equips a pre-trained VLM with a set of tools that support iterative experimentation on subcomponents of computer vision models to explain their behavior.

To the best of our knowledge, limited work has been done to investigate the functional roles of neurons in VLMs. The multi-modal nature of the input data and the intricate network structures make this a particularly distinctive and challenging domain. Stan *et al.* [28] design an interface to visualize how generated outputs of a VLM are related to the input image through raw attention, relevancy maps, and causal interpretation. [10, 22] identify neurons linked to specific semantics in an individual sample, but do not systematically analyze a neuron function across the entire dataset.

Our work globally characterizes neuron roles from token-level activations across the dataset, offering a holistic view of a neuron's behavior.

3 Method

The functions of neurons in VLMs remain largely mysterious – particularly whether they process visual and text tokens differently. Inspired by [7], we conduct analyses based on neuron activations with respect to tokens. Unlike prior work, we examine both visual and textual tokens simultaneously to gain deeper insights into the inner workings of VLMs.

Figure 2 illustrates the main workflow for investigating the functions of neurons in a VLM (e.g., LLaVA). For a sample, the VLM takes the image and a text prompt as input and outputs predicted texts. For a given neuron in the VLM and a given sample, we obtain its activations with respect to each visual and text token (see an example in Figure 1). We record the activations for the top N (e.g., $N = 50$) samples with the highest activation values (which we refer to as top-activated samples) of the dataset for further analysis. For each neuron, based on its top-activated samples and corresponding activations, the explainer automatically generates an explanation of the neuron function. The visual simulator and text simulator estimate the activations for the visual and text tokens based on the

explanation, respectively. We assess the reliability of the explanation by computing the correlation between simulated activations and actual (*i.e.*, ground-truth) activations.

Without loss of generality, we perform analyses based on a representative VLM, LLaVA-1.5 (7B). Similar trends are observed in another VLMs, such as InternVL 2.5 (8B) and Qwen2.5-VL (3B) (see Section 8 and Section 9 in the Supplementary). In particular, we reveal the existence of neurons that are responsible only for visual information, neurons that respond only to text, and neurons that are responsible for both modalities, respectively. We study the characteristics of these neurons to gain a deeper understanding of the internal workings of VLMs.

3.1 Existence of specific neurons

Rare studies explore the internal workings of VLMs capable of processing both visual and text information. This raises a compelling question: do these models contain neurons that are uniquely responsive to specific modalities?

To demystify this, we studied a large number of neurons within a VLM, observing their responses on both visual and text tokens. Our findings reveal several noteworthy patterns. 1) Some neurons exhibit a strong response to visual tokens while showing weak activations for text tokens, as illustrated in Figure 3 (a). 2) Some neurons demonstrate a high response to text tokens while exhibiting weak activations for visual tokens, as showcased in Figure 3 (b). We name these as ‘visual neurons’ and ‘text neurons’, respectively. 3) Additionally, we also found neurons that respond highly to both visual and text tokens, as depicted in Figure 3 (c)-(f). We refer to these as ‘multi-modal neurons’. For example, in (d), both the visual tokens and text tokens associated with ‘doughnuts’ trigger high activations. Interestingly, we observe that the responses to visual and text tokens typically correspond to a consistent concept.

3.2 Identifying specific neurons

Having confirmed the presence of modality-specific neurons (*i.e.*, those responsive primarily to visual or textual input) as well as multi-modal neurons, we are wondering: how can we automatically identify and localize these neurons of the large population of neurons in a VLM?

We define four categories of neurons: visual neurons, text neurons, multi-modal neurons, and unknown neurons. To classify a given neuron, we analyze its top N samples with the highest activation values (e.g., $N = 50$). Similarly to Bills et al. [7], the activations of each neuron are normalized to discrete values between 0 and 10, where the negative values are assigned to 0 and the maximum activation value of the neuron is mapped to 10.

By analyzing the activations of this neuron on the N samples, we estimate the probability of this neuron belonging to visual neuron, text neuron, multi-modal neuron, or unknown neuron as (p_v, p_t, p_m, p_u) , where $p_v + p_t + p_m + p_u = 1$. Specifically, we calculate the proportion of samples in which the neuron’s activations meet the criteria for visual, text, or multi-modal responses. In principle, a sample could be identified as visual (or text)-activated if any visual token (or text token) shows obvious activation. However, we observe that low activations (e.g., values of 1 or 2) or some isolated high activations often behave as noise or outliers. To enhance robustness,

we introduce thresholds based on extensive observation of token activations to mitigate these effects. For a given sample, if the number of visual tokens with high activations (activation value greater than $T_v = 2$) exceeds n_v ($n_v = 4$), we classify this sample as a *visual-activated sample*, indicating that this neuron is responsive to this sample’s visual tokens. Similarly, if the number of text tokens with high activations (activation value greater than $T_t = 3$) exceeds n_t ($n_t = 2$), we consider it a *text-activated sample*.

We define a sample as a *visual sample* if it is visual-activated but not text-activated. Similarly, a *text sample* is defined as one that is text-activated but not visual-activated. A *multi-modal sample* is both text-activated and visual-activated, while an *unknown sample* is neither visual-activated nor text-activated. Based on the distribution of these four types of samples, we compute the probability distribution (p_v, p_t, p_m, p_u) indicating the likelihood that the neuron belongs to each of the four corresponding neuron types. Intuitively, a higher value of p_v suggests that the neuron is more likely to be a visual neuron. Similarly, p_t, p_m , and p_u reflect the neuron’s alignment with text, multi-modal, or unknown categories, respectively. This probability distribution enables us to estimate the type of a neuron in a principled and interpretable manner. Detailed analysis is presented in the experimental section.

3.3 Explanation and simulation

Upon identifying a neuron as specialized, we further investigate the neuron’s function in representing specific concepts. For instance, if a visual neuron consistently exhibits high activations in response to visual tokens featuring “person” and low activation for other tokens, it is likely that the neuron encodes the concept of “person”. Similarly, a text neuron may exhibit selectivity and focus on particular words or positional patterns within sentences, suggesting its specialization in capturing certain linguistic concepts or functions.

Instead of relying on human interpretation to understand the function of a neuron, we develop a framework that enables automatic generation and evaluation of neuron function explanations. Bills et al. [7] propose an explanation-simulation framework using GPT-4; however, their analysis is limited to text tokens and could not handle visual and text modalities. Although GPT-4o has the ability to understand images, it cannot easily align and interpret the patched visual tokens, making simulating visual activations challenging. Designing a pipeline tailored for visual token simulation is essential for enabling reliable activation simulations, thereby facilitating the evaluation of explanation quality. As illustrated in Figure 2 (b), our framework comprises two modules: explainer and simulator.

Explainer For a given neuron, we select its top- k activated samples (uniformly sampled from the top- N activated samples, where $k < N$, to balance sample diversity and token number) along with their corresponding activation values as input to the explainer, which then generates/outputs an explanation of the neuron’s function. We use GPT-4o as the explainer. As illustrated in Figure 10 in our Supplementary, the prompt input to GPT-4o consists of a system prompt and a small number (*i.e.*, $M = 8$) of in-context examples.

Particularly, for each sample, we represent its text part by the pairs of (text token, activation) and represent the visual part by the activation-modulated image, enabling the explainer to perceive and

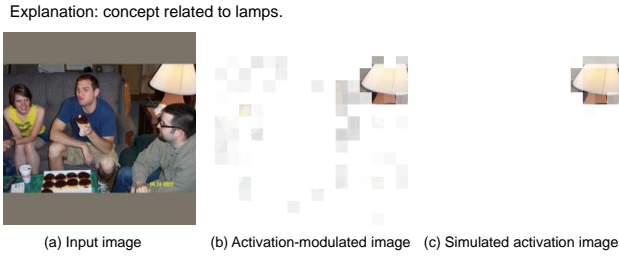


Figure 4: An example for illustrating (a) the original image, (b) its activation-modulated image of a visual neuron, and (c) the simulated activation-modulated image. Note that the explanation of this neuron is “concept related to lamps”. We can see that the image patches where the desk lamp is located are mainly activated by this visual neuron in (b), and activated by the simulator in (c).

interpret the samples. Figure 4 shows an example of (a) the image, and (b) its activation-modulated image, where the more transparent the image patch, the higher activation this visual token has.

Simulator For simulation, we have a visual simulator and a text simulator.

The *visual simulator* takes the explanation (generated by the explainer with respect to a given neuron) and the test image as input, and outputs simulated activation values for each visual token. We adopt Grounded SAM 2 [25] as our visual simulator. It outputs object mask (with values of 0 to 1) based on the concepts from the explanation and the test image. To convert the mask into activations, we scale it by a factor of 10. Given a neuron’s explanation and an input image, Figure 4 (c) shows an example of the simulated activations of a visual neuron by modulating the activation values to the original images (see Figure 8-9 for more visualization).

We use GPT-4o as the *text simulator*. Given a neuron’s explanation and a test sample, with system prompt and M in-context examples, the simulator generates activation value for each text token (see Figure 11 in our Supplementary). For a text neuron, we feed only its text input into the text simulator. For a multi-modal neuron, we provide both the image and text inputs, but instruct the text simulator to estimate just the text-token activations.

Scoring Following previous work [7], we calculate the Pearson correlation coefficient [23] between the simulated activations and actual activations to measure the degree of their correlation as the simulation score, which quantifies the quality of the generated explanation.

For a multi-modal neuron, we calculate the score for visual part and text part respectively and average them as the overall score. For a text (or visual) neuron, the score from the text (or visual) simulator is taken as its score.

4 Experiments

We conducted experiments based on LLaVA-1.5 (7B) [16]. More results based on VLMs of InternVL 2.5 (8B) [9] and Qwen2.5-VL (3B) [3] can be found in Section 8 and Section 9 in the Supplementary.

4.1 Neuron activation dataset

Here, we elaborate the details of obtaining the neuron activation dataset derived from the representative VLM, LLaVA-1.5 (7B). From the training dataset of LLaVA-1.5, we curated a dataset that includes 23k image and text pairs with detailed image descriptions (with the images sourced from the COCO2017 [14] dataset). We perform the analysis on the 23k image-text pairs.

Following [22, 29], we focus on the interpretation of neurons in the Feedforward Neural (FFN) layers, while leaving the study for attention layer as future work. Neurons within the FFNs are found to be capable of storing factual knowledge, encoding positional information, responding to particular syntactic triggers, *etc* [29]. The embedding parameters of the attention heads for calculating attention weights focus on token interactions and may do not have such capability. We use the output from the activation function of the first linear transformation (neurons) of each FFN layer as the neuron activations. During the data collection process, for each sample, an image and its text prompt are fed into LLaVA-1.5 7B [16] for inference and we record the response/activation to each token. Hence, we get *(token, activation)* pairs for this sample, where the tokens include visual tokens and text tokens.

For each neuron, we select the top $N = 50$ samples eliciting the maximum activation values (by ranking the samples based on each sample’s maximum activation value) and $N = 50$ random samples from the 23k samples for analysis. Given that LLaVA-1.5 7B comprises 32 blocks with 11,008 neurons in the FFN layer of a block, there are a total of 352,256 neurons.

4.2 Findings of neuron function

We observed responses of many neurons. We found that the neurons in a VLM are not homogeneous. There exist visual neurons, text neurons, and multi-modal neurons, which are mainly responsible only for visual tokens, text tokens, and both, respectively.

Figure 3 shows some typical examples. For visual tokens, a higher transparent degree indicates a higher activation. For text tokens, the darker of the green color indicates a higher activation. Specifically, Figure 3 (a) shows that the prominent activations of the neuron predominantly occurs in visual tokens, with low (ignorable) activations for text tokens. Such neuron is responsible for vision and we refer to it as visual neuron. As demonstrated in Figure 3 (b), the activation pattern of another neuron category shows high responses to text tokens while ignorable responses to visual tokens. These neurons are referred to as text neurons. Moreover, as presented in Figure 3 (c)-(f), a third category of neurons exhibits high activations on both visual and text tokens, underscoring their role in processing multi-modal information. We refer to them as multi-modal neurons.

For multi-modal neurons, our findings show an intriguing alignment in the response semantics to both visual and text tokens. This alignment encompasses correlations with actual objects as well as abstract states. For example, Figures 3 (c)(d) elucidate the alignment related to actual objects, demonstrating that both visual and text tokens are consistently related to the concepts of ties and donuts, respectively. Figure 3 (e) exemplifies the alignment of abstract states, where text tokens with high activation values such as walking, running, interacting, and standing, are aligned with the highly-activated image regions of zebras. Similarly, Figure

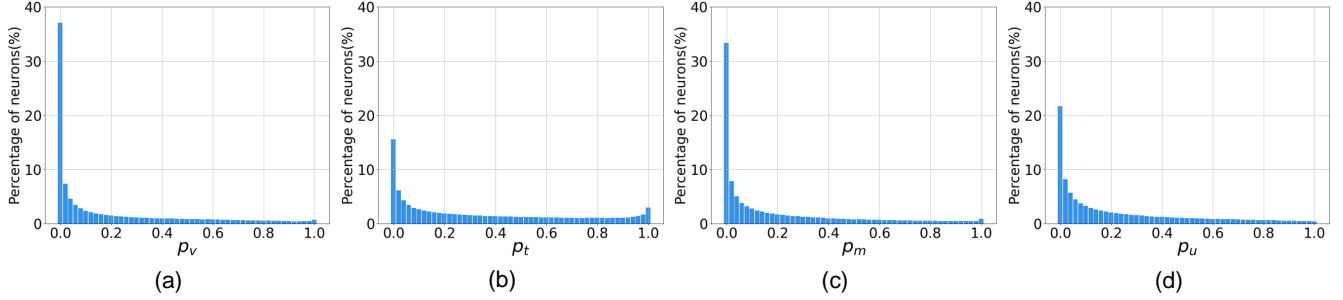


Figure 5: Histogram for the probability p_v , p_t , p_m , and p_u of belonging to visual neuron, text neuron, multi-modal neuron, and unknown neuron types, respectively.

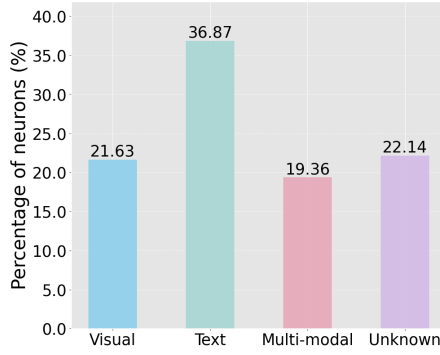


Figure 6: Distribution of the four types of neurons (visual-prone neurons, text-prone neurons, multimodal-prone neurons, unknown-prone neurons) when we treat the determination of the neuron type as a classification problem.

3 (f) showcases text tokens with pronounced activations relating to drinking, standing (referring to birds), and walking (relating to humans), alongside activated image patches depicting birds and humans. These observations show that the multi-modal neurons usually deliver aligned concepts over text and visual tokens.

Besides the three neuron types, there exist neurons that exhibit simultaneously low activations to both visual and text tokens, which we refer to as unknown neurons. Such neurons may be redundancy neurons that are not well optimized. The multifaceted functionality of neurons contributes to VLM's strong visual understanding and reasoning capability.

4.3 Distributions of different types of neurons

How can we automatically identify the type of neuron? As discussed in Section 3.2, based on the top- N highly activated samples, we can estimate the probability of belonging to the four different neuron types by (p_v, p_t, p_m, p_u) .

We show the histogram for the probability of p_v , p_t , p_m , and p_u over all the neurons, respectively in Figure 5 (a)-(d). Only a small fraction of neurons exhibit a high likelihood of belonging to a specific type. Specifically, approximately 6.0% are classified as visual neurons with over an 80% probability; 15.3% exceed this threshold for text neurons; 6.1% for multi-modal neurons; and 6.4% for unknown neurons.

When we consider the identification of neuron type as a classification problem by recognizing the type of high probability as the neuron type, we obtain the class distribution for the four types of neurons for all (352,226) neurons. As revealed in Figure 5 (a), only a small fraction of neurons can be confidently assigned to a specific type; the majority present mixed patterns. For example, a neuron may have the probability of $p_v = 0.4$, $p_t = 0.1$, $p_m = 0.3$, and $p_u = 0.2$ of being the four types. Therefore, more precisely, we refer to it as a visual-prone neuron rather than visual neuron. Figure 6 shows the distribution of the visual-prone neurons, text-prone neurons, multimodal-prone neurons, and unknown-prone neurons. The text-prone neurons have the highest frequency, while the other three types of neurons exhibit similar proportions.

4.4 Neuron distributions across layers/blocks

In this section, we explore the distribution of the four neuron types in the blocks / FFN layers of the model. For each category, we selected top 10,000 neurons ranked by the probability—approximately 2.8% of neurons per type—for our analysis. The distributions of neurons across the layers/blocks are shown in Figure 7. For visual neurons and text neurons, they present high frequency in the early and middle layers while low frequency in the high layers. In contrast, the multi-modal neurons have higher frequency in the high layers. That may because in the early and middle layers, more visual neurons and text neurons are learned to focus on processing the individual modality. In the high layers, more multi-modal neurons are learned to jointly deal with visual and text information, enabling efficient reasoning of visual and text information.

4.5 Visualization of simulation results

We visualize the simulation results for three types of neurons with different functions. For each type of neurons, we show simulation results for two samples of the same neuron.

Figure 8 shows the activations of a visual neuron with respect to two samples. When observing the actual activations (ground-truth) of both the visual and text tokens, there are predominant activations over visual tokens but negligible activations for text tokens. In addition, the predicted activations from the visual simulator are consistent with those actual activations. *Interestingly, we found that a visual neuron responds strongly to visual regions related to the neuron's concept (e.g., train-related), but shows low or*

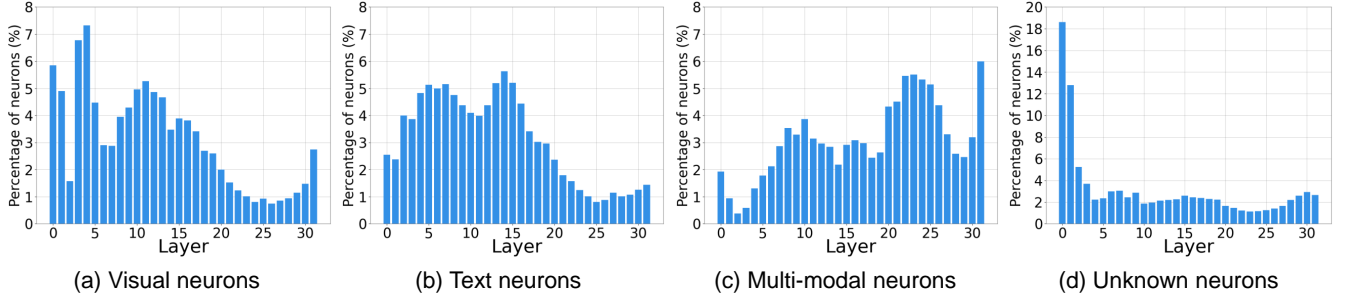


Figure 7: The distribution of special neurons over different layers. (a)-(d) show four categories of neurons, namely visual, text, multi-modal and unknown neurons. The horizontal axis denotes the model layer, from 0 to 31. The vertical axis denotes the number of neurons in the corresponding layer.

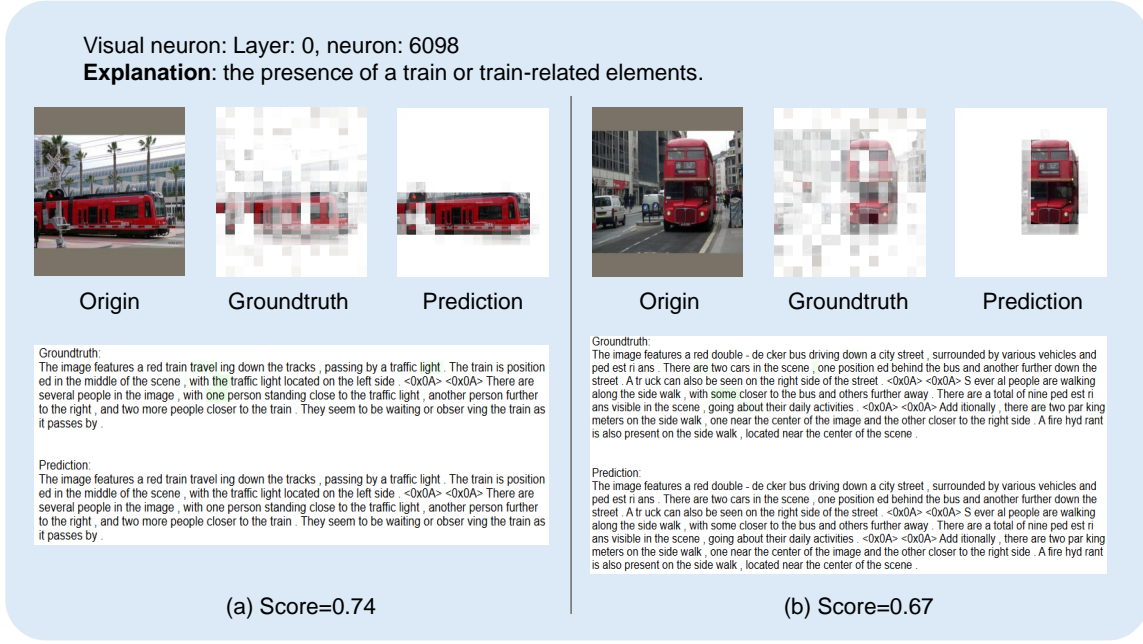


Figure 8: Visualization of actual activations and simulation results of a visual neuron.

negligible responses to text tokens, even when those tokens (e.g., train) are conceptually relevant.

Figure 9 shows the activations of a multi-modal neuron with respect to two samples. The neuron exhibited high responses to both visual and text tokens related to airplanes and airports, which is consistent with the explanation. This coherence between visual and textual responses underscores the neurons' capacity to capture information across modalities. Such findings highlight the interesting functionality of multi-modal neurons in bridging the gap between disparate modalities.

Figure 16 in the Supplementary shows some typical examples of text neurons. They in general present large activations on some text tokens while negligible activations on visual tokens.

4.6 Explanation quality

We evaluate the quality of generated explanations for different types of neurons, with each explanation generated based on the neuron's

Table 1: Explaination quality and impacts of different sampling strategies on three neuron categories.

Neuron category	Top sampling	Random sampling
Visual neurons	0.160	0.140
Text neurons	0.240	0.149
Multi-modal neurons	0.235	0.175

top activated samples. For each neuron type, we randomly selected 800 high-confidence neurons (*i.e.*, neurons whose type classification was unambiguous). As shown in Table 1, the generated explanations are scored of 0.160, 0.240, and 0.235 for visual neurons, text neurons, and multi-modal neurons, respectively.

In addition, we explore the impact of two different sampling strategies for generating explanations: the first method uniformly selects $k = 5$ samples (top 1, 5, 9, 13, 17) from the top 20 samples to elucidate the function of the neuron, while the second randomly

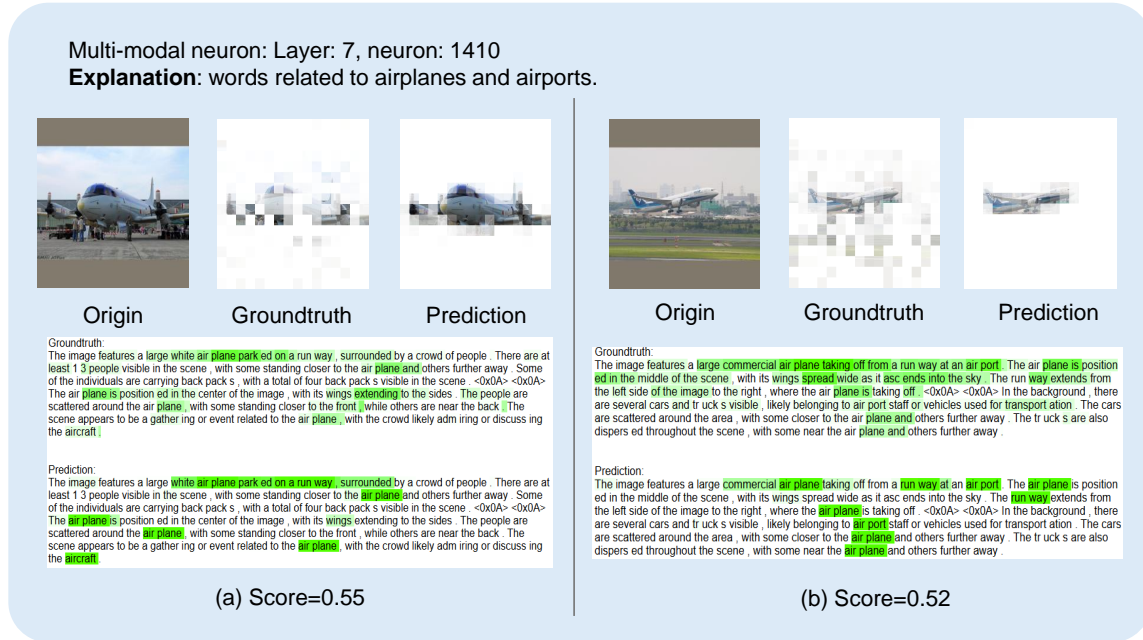


Figure 9: Visualization of actual activations and simulation results of a multi-modal neuron.

chooses five samples from the whole 23k image-text pairs. We conduct simulation of the activations on the uniformly selecting five samples (top 3, 7, 11, 15, 19) from the top 20 samples for each neuron. The more accurate the generated explanations are, the more closely the simulated activations will align with the true neuron activations, resulting in higher evaluation scores. Table 1 shows that the explanations generated from the top samples are more accurate than those of the random samples, indicating the efficiency of the sampling strategy. In addition, the gain of the top sampling over random sampling for visual neurons is not as large as that on text neurons and multi-modal neurons. The main reason is that some neurons are polysemy and present responses over multiple different concepts. However, the explainer does not fully capture all these concepts and leads to the mismatch between the simulated activations and the actual activations (see Section 7.6 in the Supplementary for the visualization).

4.7 Impact of input modality on explanation

We explore the impact of input modality on explanation quality for multi-modal neurons. We use text-only, vision-only, and both (text and vision) of the top-activated samples as the input to the explainer, respectively. Table 2 shows the simulation scores for the visual part, text part, and the overall score for each type of explanation, respectively. Incorporating vision increases the visual simulator score from 0.221 to 0.230, and the overall score improves.

4.8 Impact of pruning unknown neurons

We investigate the impact of pruning a certain unknown neurons on LVM by evaluating the performance on visual question answering (VQA) task. The results show that dropping unknown neurons

Table 2: Impact of input modality on the explanation quality for multi-modal neurons.

Input modality	Visual part	Text part	Overall score
Text-only	0.221	0.239	0.230
Vision-only	0.203	0.200	0.201
Both	0.230	0.240	0.235

brings smaller performance drop than randomly dropping neurons (see Section 7.2 in the Supplementary for more details).

4.9 Outlier neurons from multi-modal neurons

For the multi-modal neurons, we found that there are some special neurons that are strongly activated for most tokens, which we refer to outlier neurons. Such neurons do not have specific semantics but actively contribute to the generation. We conducted statistical analysis on high-confidence multi-modal neurons (where $p_m = 1$) to identify those neurons. We found there are about 5% neurons that are outlier neurons (see Section 7.3 in the Supplementary).

5 Conclusion

Our study provides new insights into the internal workings of VLMs by systematically analyzing the functions of individual neurons. Our findings reveal the presence of specialized neurons for vision, text, and multi-modal processing, which we refer them as visual neurons, text neurons, and multi-modal neurons. We developed a framework utilizing GPT-4o for automated neuron explanation and introduced an activation simulator to evaluate the reliability of explanations for visual and multi-modal neurons. Through comprehensive analysis on a representative VLM of LLaVA, we shed light on the distinct neuron behaviors and characteristics, contributing to the transparency and interpretability in VLMs.

References

- [1] Jinze Bai, Shuai Bai, Shusheng Yang, Shijie Wang, Sinan Tan, Peng Wang, Junyang Lin, Chang Zhou, and Jingren Zhou. 2023. Qwen-vl: A frontier large vision-language model with versatile abilities. *arXiv preprint arXiv:2308.12966* (2023).
- [2] Nicholas Bai, Rahul A. Iyer, Tuomas Oikarinen, Akshay Kulkarni, and Tsui-Wei Weng. 2025. Interpreting Neurons in Deep Vision Networks with Language Models. *arXiv preprint arXiv:2403.13771* (2025).
- [3] Shuai Bai, Kegin Chen, Xuejing Liu, Jialin Wang, Wenbin Ge, Sibo Song, Kai Dang, Peng Wang, Shijie Wang, Jun Tang, et al. 2025. Qwen2.5-vl technical report. *arXiv preprint arXiv:2502.13923* (2025).
- [4] David Bau, Bolei Zhou, Aditya Khosla, Aude Oliva, and Antonio Torralba. 2017. Network dissection: Quantifying interpretability of deep visual representations. In *Proceedings of the IEEE conference on computer vision and pattern recognition*. 6541–6549.
- [5] Leonard Bereska and Efstratios Gavves. 2024. Mechanistic Interpretability for AI Safety—A Review. *arXiv preprint arXiv:2404.14082* (2024).
- [6] Lucas Beyer, Andreas Steiner, André Susano Pinto, Alexander Kolesnikov, Xiao Wang, Daniel Salz, Maxim Neumann, Ibrahim Alabdulmohsin, Michael Tschanen, Emanuele Bugliarello, et al. 2024. Paligemma: A versatile 3b vlm for transfer. *arXiv preprint arXiv:2407.07726* (2024).
- [7] Steven Bills, Nick Cammarata, Dan Mossing, Henk Tillman, Leo Gao, Gabriel Goh, Ilya Sutskever, Jan Leike, Jeff Wu, and William Saunders. 2023. Language models can explain neurons in language models. *URL https://openaipublic.blob.core.windows.net/neuron-explainer/paper/index.html* (Date accessed: 14.05.2023) 2 (2023).
- [8] Kirill Bykov, Laura Kopf, Shinichi Nakajima, Marius Kloft, and Marina Höhne. 2023. Labeling neural representations with inverse recognition. *Advances in Neural Information Processing Systems* 36 (2023), 24804–24828.
- [9] Zhe Chen, Weiyun Wang, Yue Cao, Yangzhou Liu, Zhangwei Gao, Erfei Cui, Jinguo Zhu, Shenglong Ye, Hao Tian, Zhaoyang Liu, et al. 2024. Expanding performance boundaries of open-source multimodal models with model, data, and test-time scaling. *arXiv preprint arXiv:2412.05271* (2024).
- [10] Junfeng Fang, Zac Bi, Ruipeng Wang, Houcheng Jiang, Yuan Gao, Kun Wang, An Zhang, Jie Shi, Xiang Wang, and Tat-Seng Chua. 2024. Towards neuron attributions in multi-modal large language models. *Advances in Neural Information Processing Systems* 37 (2024), 122867–122890.
- [11] Leon Guertler, M Ganesh Kumar, Anh Tuu Luu, and Cheston Tan. 2024. TeLLMe what you see: Using LLMs to Explain Neurons in Vision Models. (2024).
- [12] Evan Hernandez, Sarah Schwettmann, David Bau, Teona Bagashvili, Antonio Torralba, and Jacob Andreas. 2021. Natural language descriptions of deep visual features. In *International Conference on Learning Representations*.
- [13] Junnan Li, Dongxu Li, Silvio Savarese, and Steven Hoi. 2023. Blip-2: Bootstrapping language-image pre-training with frozen image encoders and large language models. In *International conference on machine learning*. PMLR, 19730–19742.
- [14] Tsung-Yi Lin, Michael Maire, Serge Belongie, James Hays, Pietro Perona, Deva Ramanan, Piotr Dollár, and C Lawrence Zitnick. 2014. Microsoft coco: Common objects in context. In *ECCV*. Springer, 740–755.
- [15] Haotian Liu, Chunyuan Li, Yuheng Li, and Yong Jae Lee. 2023. Improved Baselines with Visual Instruction Tuning.
- [16] Haotian Liu, Chunyuan Li, Yuheng Li, and Yong Jae Lee. 2024. Improved Baselines with Visual Instruction Tuning. In *Proceedings of the IEEE/CVF Conference on Computer Vision and Pattern Recognition (CVPR)*. 26296–26306.
- [17] Haotian Liu, Chunyuan Li, Qingyang Wu, and Yong Jae Lee. 2023. Visual Instruction Tuning. In *NeurIPS*.
- [18] Muhammad Maaz, Hanoona Rasheed, Salman Khan, and Fahad Shahbaz Khan. 2023. Video-chatgpt: Towards detailed video understanding via large vision and language models. *arXiv preprint arXiv:2306.05424* (2023).
- [19] Humza Naveed, Asad Ullah Khan, Shi Qiu, Muhammad Saqib, Saeed Anwar, Muhammad Usman, Naveed Akhtar, Nick Barnes, and Ajmal Mian. 2023. A comprehensive overview of large language models. *arXiv preprint arXiv:2307.06435* (2023).
- [20] Tuomas Oikarinen and Tsui-Wei Weng. 2022. Clip-dissect: Automatic description of neuron representations in deep vision networks. *arXiv preprint arXiv:2204.10965* (2022).
- [21] Tuomas Oikarinen and Tsui-Wei Weng. 2024. Linear explanations for individual neurons. *arXiv preprint arXiv:2405.06855* (2024).
- [22] Haowen Pan, Yixin Cao, Xiaozhi Wang, and Xun Yang. 2023. Finding and editing multi-modal neurons in pre-trained transformer. *arXiv preprint arXiv:2311.07470* (2023).
- [23] K Pearson. 1895. Notes on regression and inheritance in the case of two parents proceedings of the royal society of London, Vol. 58.
- [24] Dakning Rai, Yilun Zhou, Shi Feng, Abulhai Saparov, and Ziyu Yao. 2024. A practical review of mechanistic interpretability for transformer-based language models. *arXiv preprint arXiv:2407.02646* (2024).
- [25] Tianhe Ren, Shilong Liu, Ailing Zeng, Jing Lin, Kunchang Li, He Cao, Jiayu Chen, Xinyu Huang, Yukang Chen, Feng Yan, et al. 2024. Grounded sam: Assembling open-world models for diverse visual tasks. *arXiv preprint arXiv:2401.14159* (2024).
- [26] Tamar Rott Shaham, Sarah Schwettmann, Franklin Wang, Achyuta Rajaram, Evan Hernandez, Jacob Andreas, and Antonio Torralba. 2024. A multimodal automated interpretability agent. In *Forty-first International Conference on Machine Learning*.
- [27] Chandan Singh, Jeevana Priya Inala, Michel Galley, Rich Caruana, and Jianfeng Gao. 2024. Rethinking interpretability in the era of large language models. *arXiv preprint arXiv:2402.01761* (2024).
- [28] Gabriela Ben Melech Stan, Raanan Yehezkel Rohekar, Yaniv Gurwicz, Matthew Lyle Olson, Anahita Bhiwandiwalla, Estelle Aflalo, Chenfei Wu, Nan Duan, Shao-Yen Tseng, and Vasudev Lal. 2024. LVLM-Intrepret: An Interpretability Tool for Large Vision-Language Models. *arXiv preprint arXiv:2404.03118* (2024).
- [29] Tianyi Tang, Wenyang Luo, Haoyang Huang, Dongdong Zhang, Xiaolei Wang, Xin Zhao, Furu Wei, and Ji-Rong Wen. 2024. Language-specific neurons: The key to multilingual capabilities in large language models. *arXiv preprint arXiv:2402.16438* (2024).
- [30] Feiyu Xu, Hans Uszkoreit, Yangzhou Du, Wei Fan, Dongyan Zhao, and Jun Zhu. 2019. Explainable AI: A brief survey on history, research areas, approaches and challenges. In *Natural language processing and Chinese computing*. Springer, 563–574.

6 More implementation details

In this section, we provide more implementation details of the explainer, the simulator, and scoring.

6.1 Explainer

Figure 10 shows the prompt we used for the explainer.

One may wonder why we use activation-modulated images instead of the (visual token, activation) pairs as the input to the explainer. That because GPT-4o is a black-box where the visual tokenization is not the same as the VLM to be interpreted, it is infeasible to input the visual token and activation as what the text part does. We attempted to use VQ-GAN quantized token index and activation as input to GPT-4o, but failed. The reason is that this strategy requires abundant context examples to fully capture the meaning of the indexes of VQ-GAN, where only a few context examples are far from enough to learn the reasoning capability. Abundant context examples would increase the computation burden and exceed the contextual length limitation. Note that the activation-modulated image is obtained as $(\text{pixel-value} \times \text{activation}/10 + 255 \times (1 - \text{activation}/10))$ for each color channel.

6.2 Simulator

For the text simulator, as illustrated in Figure 11, with system prompt (marked in black) and M examples (marked in green) as context, the simulator generates activation value for each text token for the input test sample.

6.3 Scoring

The Pearson correlation coefficient between X and Y is calculated as follows:

$$r_{xy} = \frac{\sum_{i=1}^n (x_i - \bar{x})(y_i - \bar{y})}{\sqrt{\sum_{i=1}^n (x_i - \bar{x})^2} \sqrt{\sum_{i=1}^n (y_i - \bar{y})^2}}, \quad (1)$$

where x_i and y_i denote the observed values of X and Y , respectively, \bar{x} and \bar{y} denote the means of X and Y , respectively, and n denotes the number of observations.

For visual neurons, since they have no response on text tokens, it is meaningless to simulate the activations and calculate the Pearson correlation coefficient between the true activations and simulated activations on text tokens. Therefore, we only calculate the Pearson correlation coefficient (score) for visual tokens. Similarly, for text neurons, we only calculate the Pearson correlation coefficient between the true activation values and the simulated activation values on text tokens. For multi-modal neurons, we calculate the Pearson correlation coefficients on visual and text tokens separately and average them as the final score.

7 More analysis on top of LLaVA-1.5

7.1 Computational cost

Recording neuron activations for 23k samples takes 32 hours on 8 A100 GPUs. With batch size as 1, explanation generation via GPT-4o takes 4.17 seconds (s) per neuron, visual simulation takes 0.21s per image, and text simulation 18.19s per sample.

7.2 Impact of pruning unknown neurons

Unknown neurons exhibit small activations in response to visual and text tokens. We investigate the impact of pruning unknown

neurons on LVM by evaluating its performance on visual question answering (VQA) task. We randomly sampled 1,000 instances from the LLaVA-Instruct-158K dataset [17] for evaluation.

Following [18], we use average accuracy/score given by GPT-4 to measure the quality of the generated answers. The accuracy is calculated based on the binary correctness given by the evaluator. A score ranging from 0 to 5 is assigned to quantify the similarity between the predicted answers and the ground truths, with higher scores indicating closer alignment.

We sequentially pruned unknown neurons by selecting neurons with high probability of being unknown neurons (*i.e.*, $p_u \geq \tau$), where we set τ as 0.9, 0.8, 0.7, and 0.6, respectively. As shown in Table 3, 3.2% to 14.5% neurons were dropped based on those thresholds. In addition, we randomly drop neurons of the same ratios for comparison as marked by “Random neurons”. Figure 12 also shows the performance curves for the two schemes. We can see that dropping/pruning unknown neurons leads to smaller performance drop than randomly dropping neurons, indicating the unknown neurons with high confidence (high p_u value) have less influence on the model performance.

7.3 Outlier neurons from multi-modal neurons

For the multi-modal neurons, we found that there are some special neurons that present strong activations on most tokens, which we refer to outlier neurons. We conducted statistical analysis on 3338 high-confidence multi-modal neurons (where $p_m = 1$) to identify those neurons. Since we define an outlier neuron as a neuron that prescribes high activations for most tokens, it would have high activations for a randomly sampled sample. In contrast, a semantic meaningful multi-modal neuron in general has very low responses for randomly sampled samples since these samples in general have no related concepts for that neuron. Therefore, we judge whether a neuron is an outlier neuron by analyzing the activations of 50 randomly sampled samples. Whenever more than $r_v = 50\%$ visual tokens and more than $r_t = 50\%$ text tokens are activated for a sample, we think that this sample is activated for most tokens. When all the 50 samples are activated for most tokens, we consider this neuron as an outlier neuron. We plotted the distributions of the multi-modal neurons as the ratio r_v and r_t increases from 10% to 90% in Figure 13 (a) - (i), respectively. The horizontal axis denotes the percentage of samples that are most activated of the 50 samples. The distribution exhibits a clear bimodal pattern, with most neurons clustered near 0 and a smaller peak near 1. There are about 5% neurons that are outlier neurons among the multi-modal neurons when r_v and r_t is 30%. In addition, the distribution is not sensitive to r_v and r_t (when r_v and r_t range from 30% to 80%) and the proportion of outlier neurons ranges from 5.4% to 3.4%.

7.4 Ablation on the explainer: using raw images v.s. activation-modulated images

For the explainer, we provide contextual examples to enable its explanation capability. To facilitate the awareness of visual token activations for the explainer, we use activation-modulated images as input instead of the original image. We compare the performance of the two manners. The results in Table 4 reveal that using the

Table 3: Comparison of dropping/pruning unknown neurons and randomly dropping neurons on the visual question answering task. w/o $p_u \geq \tau$ represents pruning unknown neurons that having probability of being unknown neurons larger than τ . Performance is measured by accuracy/score. Full model represents the VQA performance without pruning. “Random neurons” denotes randomly dropping neurons of the same ratio.

	Full model	w/o $p_u \geq 0.9$	w/o $p_u \geq 0.8$	w/o $p_u \geq 0.7$	w/o $p_u \geq 0.6$
Pruning ratio (%)	0.0	3.2	6.4	10.2	14.6
Unknown neurons (Acc./Score)	65.6/3.46	64.1/3.40	61.3/3.37	60.3/3.32	58.9/3.26
Random neurons (Acc./Score)	65.6/3.46	62.9/3.37	57.7/3.24	55.9/3.18	54.3/3.14

Table 4: Effects of different input (original images, activation-modulated images, both) to the explainer on the explanation for visual neurons.

Input for explanation	Top sampling
Image	0.144
Image+activation modulated image	0.131
Activation modulated image	0.160

activation-modulated images yields a superior simulation score than that of using original images. It also outperforms the use of both the original images and activation-modulated images. The original image introduces neuron-irrelevant information that may mislead the explanation.

We also show visualization analysis in Figure 14. In Figure 14 (a), with all the five raw images depict indoor scenes, the explanation generated by the explainer is “things related to indoor settings or rooms”. In contrast, by using activation-modulated images, the explainer gives a more reasonable explanation “things related to lamps”. Similarly, in Figure 14 (b), being aware that the neuron is mainly activated related to the concept of “people”, the explainer provides more reasonable explanation “people holding or interacting with objects”.

7.5 More visualization of simulation results

In Figure 15-17, we present more visualization of visual, text and multi-modal neurons, respectively. We can see that the visual neurons exhibit large activations on some visual tokens, with negligible activations on text tokens. Text neurons have large activations on some text tokens while negligible activations on visual tokens. Multi-modal neurons, on the other hand, demonstrated significant responses to both visual and text tokens, with the represented concepts being aligned across both modalities. In Figure 16 (a1)(a2), we observed a consistently high activation for the first word in each sentence, which aligns with the explanation generated by the explainer.

Moreover, we observe that the predicted activations are consistent with the groundtruth activations, indicating the reliability of the generated explanations from the explainer. The explanations are accurate and consistent with human’s understanding.

7.6 Visualization of failure case on explanation

In Table 1, the gain of the top sampling over random sampling for visual neurons is not as large as that on text neurons and multi-modal

neurons. The main reason is that some neurons are polysemanticity and present responses over multiple different concepts. However, the explainer does not fully capture all these concepts and leads to the mismatch between the simulated activations and the actual activations. Figure 18 shows an example of polysemous visual neuron. The explanation is “related to sports and athletic activities”, while the top 5 activated samples contain an example about food. The explainer failed to cover all the concepts of the neuron.

7.7 Neuron monosemanticity and polysemanticity

We found that different neurons exhibit different characteristics. Some neurons are prone to monosemanticity, while some are prone to polysemanticity. Monosemantic neurons’ responses are prone to be highly specific, with each neuron reacting to a particular concept or piece of information. Polysemous neurons display a more complex behavior pattern, capable of responding to a multitude of different concepts simultaneously.

We analyze by observing the top 50 samples of the maximum activation value of the neuron. Figure 19 (a) shows the activations of a monosemantic neuron. For different input images, this neuron has a higher activation value only on the image patches related to the lamp. Figure 19 (b) shows the activations of a polysemantic neuron, where some images have high responses to people (the first two rows) while some images have high responds to the bracket (the last row).

For text neurons, some neurons are monosemantic. As shown in Figure 20 (a), this neuron focus on “the beginning of sentences or paragraphs”. In Figure 20 (b), the first two examples show that the neuron has high responses mainly on the text tokens “There are” and “The table”, while in the last example the neuron is activated on the words “laptop”, “monitor” and “mouse”. This indicates that the neuron is polysemantic.

For multi-modal neurons, Figure 21 (a) shows a monosemantic multi-modal neuron that is activated related to the concepts “airplane” and “airport” on both visual tokens and text tokens. Figure 21 (b) shows a polysemantic multi-modal neuron that responds highly to both donuts and carrots.

Sometimes, monosemanticity and polysemanticity cannot be clearly distinguished, since a couple of concepts could be summarized by a higher-level concept. For example, “airplane” and “airport” can be considered as two different concepts or as a concept related to “aviation”.

Prompt for explanation

We are studying neurons in a neural network. Each neuron looks for some particular thing in an image and a short document, which includes a picture and text tokens. Look at the parts of the document the neuron activates for and summarize in a single sentence what the neuron is looking for. Don't list examples of words.

The activation format is token<tab>activation. Activation values range from 0 to 10. A neuron finding what it's looking for is represented by a non-zero activation value. The higher the activation value, the stronger the match.

Example 1:

<Activation-modulated image of example 1>

<start>

The	0
man	0
is	0
we	0
aring	0
a	1
tie	4

...

<end>

Explanation of example 1 behavior: the main thing this neuron does is find words related to suits and ties.

...

Example M:

<image of example M>

...

Neuron X sample 1:

<Activation-modulated image of sample 1>

<start>

The	0
Image	0
features	1
an	0
air	4
port	7
scene	3

...

<end>

...

Neuron X sample k:

<image of sample k>

...

Explanation of neuron X behavior: the main thing this neuron does is to find

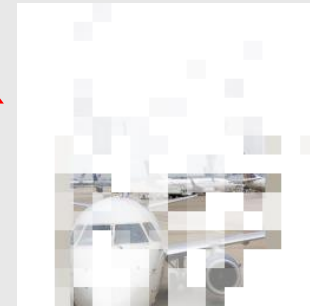
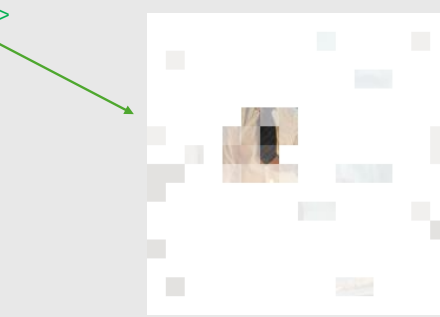


Figure 10: The prompt we used for the explainer. The system prompt is marked in black. We provide $M=8$ examples (as marked in green) as the in-context examples to enable the explainer to learn the task. Given a neuron to be explained, we input the selected top $k=5$ activated samples with each sample represented by the activation-modulated image, text tokens and text token activations (marked in red). The explainer outputs the explanation to the neuron.

Prompt for simulation

We're studying neurons in a neural network. Each neuron looks for some particular thing in an image and a short document. Look at summary of what the neuron does, and try to predict how it will fire on each token.

The activation format is token<tab>activation, activations go from 0 to 10, "unknown" indicates an unknown activation. Most activations will be 0.

Please extract tokens and unknowns based on the string input (in the format of token<tab>activation<newline>). Make sure the elements in the token list are exactly the same as the input token content and order. Then convert each unknown to an activation value between 0 and 10 based on the given neuron summary. Make sure do not miss text tokens.

Example 1:

Explanation of example 1: the main thing this neuron does is find words related to suits and ties.

<Image of example 1>

<start>

The	unknown
man	unknown
is	0
we	0
aring	0
a	1
tie	4

...

<end>

...

<image of example M>

Example M:

...

Neuron X:

Explanation of neuron X: the main thing this neuron does is find things related to airplanes and airports.

<Image of sample 1>

<start>

a	unknown
large	unknown
white	unknown
air	unknown
plane	unknown
park	unknown
ed	unknown

...

<end>



Figure 11: The prompt we used for the text simulator. The system prompt is marked in black. We provide $M=8$ examples (marked in green) as the contextual examples to enable the simulator to learn the task. Given a testing sample, the simulator turns each 'unknown' character of the text tokens to an activation value (an integer from 0-10) based on the explanation and prompt. Note that as example here, both images, and text tokens are used as input for multi-modal neurons. For text neurons, we could exclude images from the inputs to reduce taken consumption.

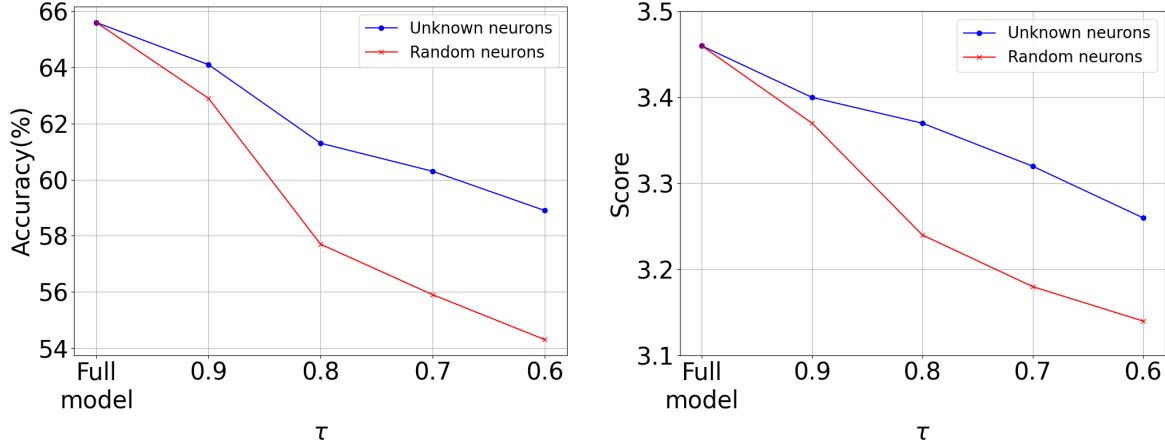


Figure 12: Comparison of dropping unknown neurons and randomly dropping neurons on the visual question answering task.

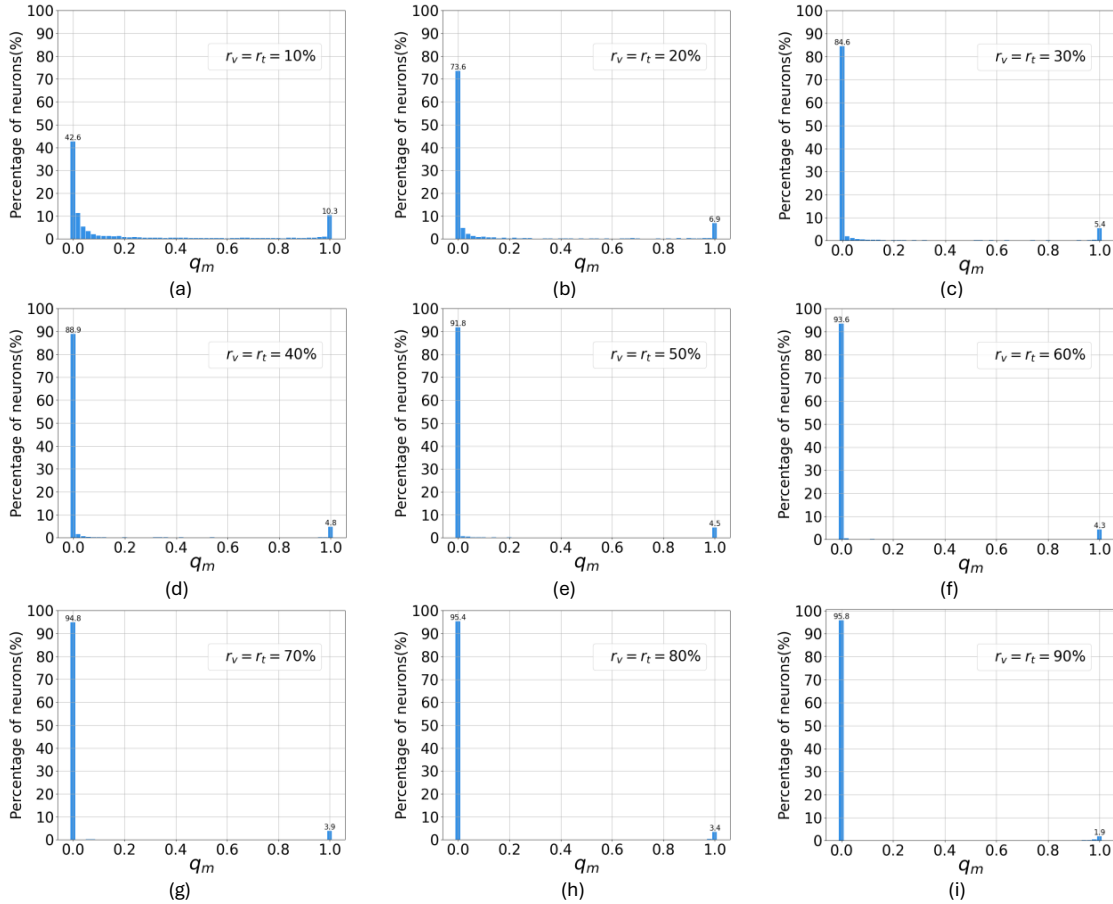


Figure 13: (a) - (i) are the distribution of multi-modal neurons with ratio r_v and r_t ranging from 10% to 90%, respectively. Horizontal axis (q_m) denotes the percentage of samples that are most activated of the 50 samples while y-axis denotes the percentage of neurons at each given q_m . The distribution exhibits a clear bimodal pattern, with most neurons clustered near 0 and a smaller peak near 1. The outlier neurons with higher q_m can be distinguished from other multi-modal neurons.

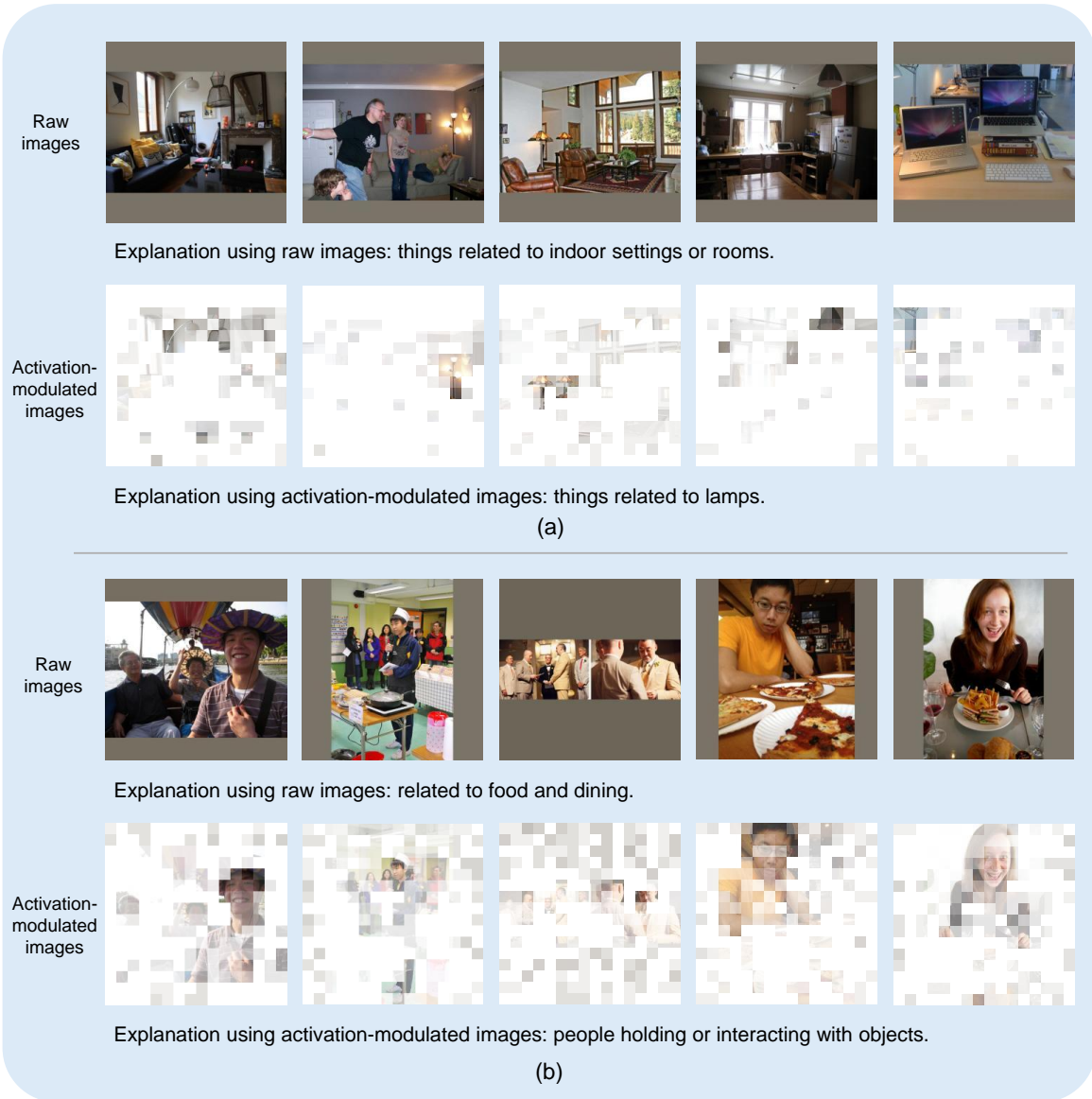


Figure 14: Visualization of the impact of using original images versus using activation-modulated images as the explainer input during the explanation step. Here we use visual neurons as examples. (a) The generated explanation using original images is “things related to indoor settings or rooms”. In contrast, The generated explanation using the activation-modulated images is “things related to lamps”, which is more adhere to the visual activations.

Visual neuron: Layer: 2, neuron: 8997

Explanation: scenes depicting groups of people gathered together.

Origin



Groundtruth



Prediction



Origin



Groundtruth



Prediction

Groundtruth:

The image features two men sitting at a dining table, eating a meal together. Both men are eating hot dogs, with one man eating a hot dog on a bun and the other man eating a hot dog with a bun and mustard. The table is set with various items, including a cup, a fork, a knife, and a spoon. The scene appears to be a gathering or event where people are standing around and engaged in conversations. One of the tables is located near the left edge of the image, while the other is situated in the background. There are also two chairs in the scene, one near the main dining table and the other near the smaller dining table.

Prediction:

The image features two men sitting at a dining table, eating a meal together. Both men are eating hot dogs, with one man eating a hot dog on a bun and the other man eating a hot dog with a bun and mustard. The table is set with various items, including a cup, a fork, a knife, and a spoon. The scene appears to be a gathering or event where people are standing around and engaged in conversations. One of the tables is located near the left edge of the image, while the other is situated in the background. There are also two chairs in the scene, one near the main dining table and the other near the smaller dining table.

(a1) Score=0.66

Groundtruth:

The image features a man wearing a red helmet and a plaid shirt, talking on his cell phone while standing in a crowd of people. The crowd consists of various individuals, some of whom are also wearing helmets. The scene appears to be a gathering or event where people are standing around and engaged in conversations. In the background, there are two bicycles, one located on the left side of the image and the other on the right side. Additionally, there are two bottles visible in the scene, one near the center and the other towards the right side.

Prediction:

The image features a man wearing a red helmet and a plaid shirt, talking on his cell phone while standing in a crowd of people. The crowd consists of various individuals, some of whom are also wearing helmets. The scene appears to be a gathering or event where people are standing around and engaged in conversations. In the background, there are two bicycles, one located on the left side of the image and the other on the right side. Additionally, there are two bottles visible in the scene, one near the center and the other towards the right side.

(a2) Score=0.62

Visual neuron: Layer: 16, neuron: 4347

Explanation: words related to roads, pathways, or walkways.

Origin



Groundtruth



Prediction



Origin



Groundtruth



Prediction

Groundtruth:

The image features a large outdoor dining area with several red chairs and dining tables arranged in a circular formation. The chairs are placed around the tables, creating a comfortable and inviting atmosphere for guests. The tables are set with plates, forks, knives, and knives, indicating that the area is prepared for a meal. In addition to the dining area, there are a few plants placed throughout the scene, adding a touch of greenery and enhancing the ambience. The outdoor dining area is surrounded by a fence, providing a sense of privacy and seclusion.

Prediction:

The image features a large outdoor dining area with several red chairs and dining tables arranged in a circular formation. The chairs are placed around the tables, creating a comfortable and inviting atmosphere for guests. The tables are set with plates, forks, knives, and knives, indicating that the area is prepared for a meal. In addition to the dining area, there are a few plants placed throughout the scene, adding a touch of greenery and enhancing the ambience. The outdoor dining area is surrounded by a fence, providing a sense of privacy and seclusion.

(b1) Score=0.60

Groundtruth:

The image depicts a group of people standing on a sidewalk, waiting to board a bus. Among them, a man is holding a skateboard, possibly preparing to ride it once he reaches his destination. The bus is visible in the background, occupying a significant portion of the scene. There are numerous people in the scene, with some standing closer to the bus and others further away. A few individuals are carrying backpacks, with one person holding a backpack near the center of the scene and another person wearing a backpack on the right side. The overall atmosphere suggests a busy and bustling public transportation environment.

Prediction:

The image depicts a group of people standing on a sidewalk, waiting to board a bus. Among them, a man is holding a skateboard, possibly preparing to ride it once he reaches his destination. The bus is visible in the background, occupying a significant portion of the scene. There are numerous people in the scene, with some standing closer to the bus and others further away. A few individuals are carrying backpacks, with one person holding a backpack near the center of the scene and another person wearing a backpack on the right side. The overall atmosphere suggests a busy and bustling public transportation environment.

(b2) Score=0.51

Visual neuron: Layer: 3, neuron: 8142

Explanation: references to food, particularly cakes and desserts.

Origin



Groundtruth



Prediction

Groundtruth:

The image features a man and a woman standing next to a dining table, both holding a large sheet cake with a flag design on it. They are in the process of cutting the cake together, likely celebrating a special occasion. There are several other people in the scene, some of them standing near the table and others further away. A knife is visible on the table, being used to cut the cake. Additionally, there are a few cups placed around the table, possibly containing beverages for the guests.

Prediction:

The image features a man and a woman standing next to a dining table, both holding a large sheet cake with a flag design on it. They are in the process of cutting the cake together, likely celebrating a special occasion. There are several other people in the scene, some of them standing near the table and others further away. A knife is visible on the table, being used to cut the cake. Additionally, there are a few cups placed around the table, possibly containing beverages for the guests.

(c1) Score=0.44



Origin



Groundtruth



Prediction

Groundtruth:

The image features a group of children gathered around a dining table, excitedly waiting for a birthday cake to be cut. A young boy is standing in front of the cake, holding a knife and preparing to cut it. The other children are eagerly watching the cake-cutting process. There are several children in the scene, with some standing closer to the table and others further away. A potted plant can be seen in the background, adding a touch of greenery to the room. The atmosphere is lively and joyful, as the children anticipate the delicious treat.

Prediction:

The image features a group of children gathered around a dining table, excitedly waiting for a birthday cake to be cut. A young boy is standing in front of the cake, holding a knife and preparing to cut it. The other children are eagerly watching the cake-cutting process. There are several children in the scene, with some standing closer to the table and others further away. A potted plant can be seen in the background, adding a touch of greenery to the room. The atmosphere is lively and joyful, as the children anticipate the delicious treat.

(c2) Score=0.31

Figure 15: Visualization of actual activations and simulation results of three visual neurons.

Text neuron: Layer: 29, neuron: 7693

Explanation: the beginning of sentences or paragraphs.

Origin



Groundtruth



Prediction

Groundtruth:
The image features a large body of water with a beautiful view of a city skyline in the background. The water is calm, and there are several boats of various sizes scattered throughout the scene. Some boats are closer to the shore, while others are further out in the water. In addition to the boats, there are several birds flying or resting in the area. Some birds are close to the water, while others are flying higher in the sky. The combination of the boats, birds, and city skyline creates a serene and picturesque scene.

Prediction:
The image features a large body of water with a beautiful view of a city skyline in the background. The water is calm, and there are several boats of various sizes scattered throughout the scene. Some boats are closer to the shore, while others are further out in the water. In addition to the boats, there are several birds flying or resting in the area. Some birds are close to the water, while others are flying higher in the sky. The combination of the boats, birds, and city skyline creates a serene and picturesque scene.

(a1) Score=0.89

Origin



Groundtruth



Prediction

Groundtruth:
The image features a festive display of teddy bears and other stuffed animals in a store. The teddy bears are arranged in various positions, with some sitting on top of each other and others placed on a table. The display is adorned with Christmas lights, creating a warm and inviting atmosphere. There are several people in the scene, with one person standing near the left side of the image, another person in the middle, and a third person on the right side. They seem to be browsing the store and admiring the teddy bear display.

Prediction:
The image features a festive display of teddy bears and other stuffed animals in a store. The teddy bears are arranged in various positions, with some sitting on top of each other and others placed on a table. The display is adorned with Christmas lights, creating a warm and inviting atmosphere. There are several people in the scene, with one person standing near the left side of the image, another person in the middle, and a third person on the right side. They seem to be browsing the store and admiring the teddy bear display.

(a2) Score=0.75

Text neuron: Layer: 20, neuron: 2063

Explanation: situations or contexts related to resting or breaks during sports activities.

Origin



Groundtruth



Prediction

Groundtruth:
The image captures a tennis match in progress, with a man in a white shirt and shorts swinging a tennis racket on a grass court. He is in the middle of a serve, and the tennis ball is visible in the air. There are several other people in the scene, likely spectators or fellow players, watching the match unfold. Some of them are standing close to the court, while others are further away. A chair can be seen near the court, possibly for resting or for the players to use during breaks.

Prediction:
The image captures a tennis match in progress, with a man in a white shirt and shorts swinging a tennis racket. He is in the middle of a serve, and the tennis ball is visible in the air. There are several other people in the scene, likely spectators or fellow players, watching the match unfold. Some of them are standing close to the court, while others are positioned further away. A chair can be seen near the court, possibly for resting or for the players to use during breaks.

(b1) Score=0.70



Origin



Groundtruth



Prediction

Groundtruth:
The image captures a tennis match in progress, with a tennis player in a white shirt and white hat standing on the court, holding a tennis racket. The player appears to be preparing to serve the ball. There are several other people in the scene, likely spectators or fellow players, watching the match. Some of them are standing close to the tennis player, while others are positioned further away. A chair can be seen in the background, possibly for the players to rest during breaks.

Prediction:
The image captures a tennis match in progress, with a tennis player in a white shirt and white hat standing on the court, holding a tennis racket. The player appears to be preparing to serve the ball. There are several other people in the scene, likely spectators or fellow players, watching the match. Some of them are standing close to the tennis player, while others are positioned further away. A chair can be seen in the background, possibly for the players to rest during breaks.

(b2) Score=0.59

Text neuron: Layer: 6, neuron: 5298

Explanation: references to the position or location of objects within an image.

Origin



Groundtruth



Prediction

Groundtruth:
The image is a collage of various food items, showcasing a diverse assortment of dishes. There are several bowls and cups scattered throughout the collage, each containing different types of food. Some of the bowls are filled with pasta, while others contain vegetables or other ingredients. The cups are filled with various liquids. In addition to the bowls and cups, there are several spoons and forks scattered throughout the collage, indicating that these utensils are used for serving and eating the food. The collage also features a couple of cakes, one of which is placed in the upper right corner, and the other in the lower left corner.

Prediction:
The image is a collage of various food items, showcasing a diverse assortment of dishes. There are several bowls and cups scattered throughout the collage, each containing different types of food. Some of the bowls are filled with pasta, while others contain vegetables or other ingredients. The cups are filled with various liquids. In addition to the bowls and cups, there are several spoons and forks scattered throughout the collage, indicating that these utensils are used for serving and eating the food. The collage also features a couple of cakes, one of which is placed in the upper right corner, and the other in the lower left corner.

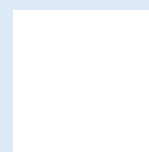
(c1) Score=0.52



Origin



Groundtruth



Prediction

Groundtruth:
The image features a delicious-looking ham burger sandwich sitting on a dining table. The sandwich is made up of a ham burger patty, a bun, and lettuce, all placed on a bun. The sandwich is accompanied by a drink in a cup, which is positioned near the top right corner of the table.

Prediction:
The image features a delicious-looking ham burger sandwich sitting on a dining table. The sandwich is made up of a ham burger patty, a bun, and lettuce, all placed on a bun. The sandwich is accompanied by a drink in a cup, which is positioned near the top right corner of the table.

(c2) Score=0.46

Figure 16: Visualization of actual activations and simulation results of three text neurons.

Multi-modal neuron: Layer: 24, neuron: 8912

Explanation: references to rivers and water bodies.

Origin



Groundtruth



Prediction



Origin



Groundtruth



Prediction

Groundtruth:

The image features a herd of elephants gathered in a body of water, possibly a river or a lake. There are at least 13 elephants in the scene, with some standing in the water and others on the shore. The elephants are of various sizes, indicating a mix of adults and younger members of the herd. <0xA> <0xA> The elephants are spread out across the water, with some closer to the foreground and others further back. They seem to be enjoying their time in the water, possibly cooling off or socializing with each other. The scene captures the beauty and tranquility of these majestic creatures in their natural habitat.

Prediction:

The image features a herd of elephants gathered in a body of water, possibly a river or a lake. There are at least 13 elephants in the scene, with some standing in the water and others on the shore. The elephants are of various sizes, indicating a mix of adults and younger members of the herd. <0xA> <0xA> The elephants are spread out across the water, with some closer to the foreground and others further back. They seem to be enjoying their time in the water, possibly cooling off or socializing with each other. The scene captures the beauty and tranquility of these majestic creatures in their natural habitat.

(a1) Score=0.62

(a2) Score=0.54

Multi-modal neuron: Layer: 23, neuron: 6568

Explanation: animals, particularly focusing on birds and large mammals.

Origin



Groundtruth



Prediction



Origin



Groundtruth



Prediction

Groundtruth:

The image features a brown and white bird, possibly a falcon, perched on a wooden bench. The bird is standing on the bench, capturing the attention of several people who are watching it. There are at least nine people in the scene, some of them standing close to the bench while others are further away. <0xA> <0xA> In addition to the people and the bird, there are a few objects in the scene. A bottle can be seen on the ground, and a handbag is placed nearby. A chair is also present in the background, and a clock is mounted on the wall.

Prediction:

The image features a brown and white bird, possibly a falcon, perched on a wooden bench. The bird is standing on the bench, capturing the attention of several people who are watching it. There are at least nine people in the scene, some of them standing close to the bench while others are further away. <0xA> <0xA> In addition to the people and the bird, there are a few objects in the scene. A bottle can be seen on the ground, and a handbag is placed nearby. A chair is also present in the background, and a clock is mounted on the wall.

(b1) Score=0.46

(b2) Score=0.43

Multi-modal neuron: Layer: 23, neuron: 844

Explanation: references to trains and train-related settings.

Origin



Groundtruth



Prediction



Origin



Groundtruth



Prediction

Groundtruth:

The image features a small red and blue train traveling down a track, likely a miniature train ride for children. The train is carrying several passengers, with at least 12 people visible on board. The train is moving along the track, providing a fun and entertaining experience for the passengers. <0xA> <0xA> In the background, there are several cars parked, indicating that the train ride is located near a park area or a busy street. The scene captures the excitement and joy of a miniature train ride, attracting the attention of both children and adults alike.

Prediction:

The image features a small red and blue train traveling down a track, likely a miniature train ride for children. The train is carrying several passengers, with at least 12 people visible on board. The train is moving along the track, providing a fun and entertaining experience for the passengers. <0xA> <0xA> In the background, there are several cars parked, indicating that the train ride is located near a park area or a busy street. The scene captures the excitement and joy of a miniature train ride, attracting the attention of both children and adults alike.

(c1) Score=0.46

(c2) Score=0.54

Figure 17: Visualization of actual activations and simulation results of three multi-modal neurons.



Figure 18: An example of polysemous visual neuron. The explanation is “related to sports and athletic activities”, while the top 5 activated samples contain an example about food. The explainer failed to cover all the concepts of the neuron.

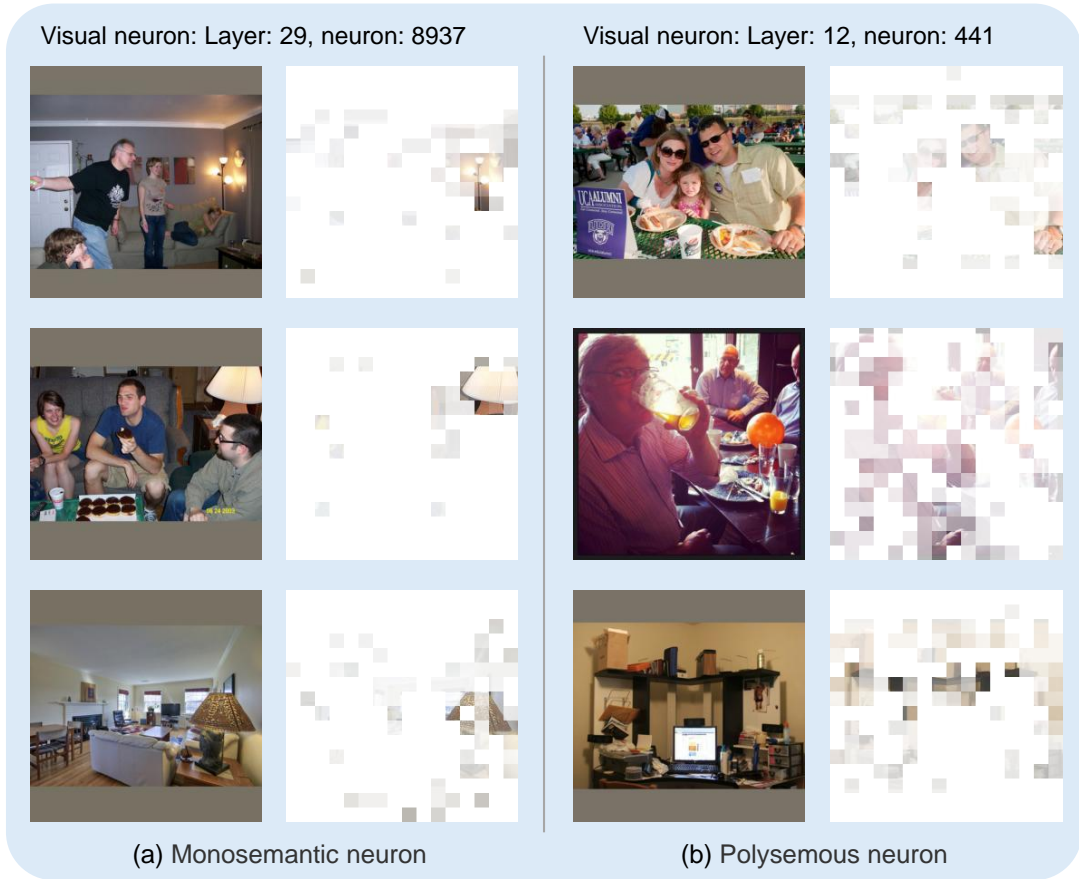


Figure 19: Examples for observing the monosemanticity or polysemanticity of visual neurons. (a) A monosemantic visual neuron, where its top 50 samples with the largest activation responses mainly are activated over the region related to lamps. Note we only show three images here to save space. (b) A polysemantic visual neuron that responds highly to both the concepts of people (the first two rows) and bracket (the last rows).

Text neuron: Layer: 29, neuron: 7693

The image depicts a bustling shopping mall with a large atrium, featuring a three-story glass ceiling. The mall is filled with numerous people walking around and exploring the various shops. There are at least 13 people visible in the scene, some of them carrying handbags. In addition to the people, there are several blackicycles scattered throughout the mall, with a total of 5 blackicycles visible. These blackicycles are likely used by visitors for transportation or as a means of exploring the mall. The overall atmosphere of the mall is lively and filled with activity.

The image features a large body of water with a beautiful view of a city skyline in the background. The water is calm, and there are several boats of various sizes scattered throughout the scene. Some boats are closer to the shore, while others are further out in the water. In addition to the boats, there are several birds flying or resting in the area. Some birds are close to the water, while others are flying higher in the sky. The combination of the boats, birds, and city skyline creates a serene and picturesque scene.

The image features a festive display of teddy bears and other stuffed animals in a store. The teddy bears are arranged in various positions, with some sitting on top of each other and others placed on a table. The display is adorned with Christmas lights, creating a warm and inviting atmosphere. There are several people in the scene, with one person standing near the left side of the image, another person in the middle, and a third person on the right side. They seem to be browsing the store and admiring the teddy bear display. In addition to the teddy bears, there are a few handbags placed around the store, possibly for sale or as part of the display.

(a) Monosemantic neuron

Text neuron: Layer: 13, neuron: 4170

The image depicts a family gathered around a dining table, enjoying a meal together. There are three people in the scene, with a young boy sitting at the table and an adult on each side of him. The table is set with various utensils, including forks, knives, and spoons, as well as multiple cups and wine glasses. <0x0A> <0x0A> In addition to the table, there are several pizzaz, indicating that the meal is likely a casual and enjoyable gathering. The chairs surrounding the table are placed at different angles, creating a comfortable and inviting atmosphere for the family to share their meal and spend quality time together.

The image depicts a group of people gathered around a dining table, enjoying a meal together. There are three people sitting at the table, with one man standing near the table, possibly serving drinks. The table is set with various items, including wine glasses, cups, and a bottle. <0x0A> <0x0A> There are multiple wine glasses placed around the table, with some closer to the people and others further away. A few cups can also be seen on the table, along with a bowl and a spoon. The table is adorned with several pizzaz, adding a touch of elegance to the scene. <0x0A> <0x0A> In the background, there is a potted plant, and a chair is visible near the table. The atmosphere appears to be relaxed and social, with everyone enjoying their time together.

The image features a desk with a laptop and a desktop computer set up. The laptop is placed on the left side of the desk, while the desktop computer is on the right side. A monitor is also present on the left side of the desk, likely connected to the desktop computer. <0x0A> <0x0A> There are two keyboards on the desk, one in front of the laptop and another in front of the desktop computer. A mouse can be seen on the right side of the desk, close to the desktop computer. <0x0A> <0x0A> In addition to the computer equipment, there are several books scattered around the desk, with some placed near the laptop and others near the desktop computer. A cup is also visible on the desk, likely for holding a beverage while working.

(b) Polysemous neuron

Figure 20: Examples for observing the monosemanticity or polysemaniticity of text neurons. (a) A monosemantic text neuron, which focuses on “the words at the beginning of a sentence or paragraph”. (b) A polysemantic text neuron, where that the first two examples show that the neuron has high responses mainly on the text tokens “There are” and “The table”, while in the last example the neuron is activated on the words “laptop”, “monitor” and “mouse”.

Text neuron: Layer: 7, neuron: 1410

The image features an airport scene with several air planes parked on the tarmac. One of the air planes is a large commercial jet, and it appears to be the main focus of the scene. The jet is parked on the runway, and there are other air planes in the background, both near and farther away. <0x0A> <0x0A> There are a few people scattered around the scene, likely airport staff or passengers. One person is standing near the large jet, while another person is located closer to the center of the image. Additionally, there is a person standing near the right edge of the scene.

The image features a large blue and white air plane parked on the runway at an airport. The air plane is positioned in the middle of the scene, with its nose pointing towards the left side of the image. Another air plane can be seen in the background, slightly to the left of the main air plane. <0x0A> <0x0A> There are several people scattered around the scene, likely airport staff or passengers. Some are standing near the main air plane, while others are positioned closer to the background air plane. A truck is also visible in the background, likely used for airport operations or maintenance.

The image features an airport scene with several air planes parked on the tarmac. There are three air planes in the scene, with one large United Airlines jet liner taking up a significant portion of the image. Another air plane is visible in the background, and a third one can be seen further away. <0x0A> <0x0A> There are numerous people scattered around the tarmac, likely working on the planes or waiting for their flights. Some of them are closer to the air planes, while others are further away. <0x0A> <0x0A> In addition to the air planes, there are several trucks and cars on the tarmac, likely providing support services for the planes. A suit case can also be seen near the center of the image, possibly belonging to a passenger or an air port worker.

(a) Monosemantic neuron

Text neuron: Layer: 31, neuron: 1800

The image features a man and a woman standing in front of a doughnut machine, which is filled with a variety of doughnuts. The man is reaching for a doughnut, while the woman is also present in the scene, likely observing or waiting for her turn to get a doughnut. <0x0A> <0x0A> In the background, there are two cars parked, one on the left side and the other on the right side of the scene. Additionally, there is a truck parked further back on the right side.

The image depicts a man working in a kitchen to prepare doughnuts. He is standing in front of a conveyor belt filled with doughnuts, which are being made and prepared for sale. The doughnuts are in various stages of the process, with some closer to the man and others further away. <0x0A> <0x0A> There are numerous doughnuts on the conveyor belt, some closer to the man and others further away. The doughnuts are arranged in a way that they are easily accessible for the man to work on. The scene captures the essence of a busy bakery, with the man ensuring that the doughnuts are made to perfection.

The image features a person standing in a kitchen, preparing a meal. They are in the process of cutting and peeling carrots, which are spread out on a dining table. The person is using a knife to carefully cut the carrots, and there are several carrots in various stages of preparation. <0x0A> <0x0A> In the kitchen, there is a microwave oven on the counter top, and a bowl can be seen nearby. The person is focused on their task, creating a healthy and delicious meal.

(b) Polysemous neuron

Figure 21: Examples for observing the monosemanticity or polysemaniticity of multi-modal neurons. (a) A monosemantic multi-modal neuron, which is activated related to the concepts “airplane” and “airport” on both visual tokens and text tokens. (b) A polysemantic multi-modal neuron, which responds highly to both donuts and carrots.

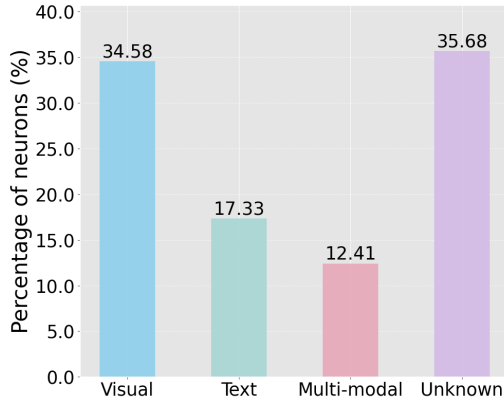


Figure 22: Distribution of the four types of neurons (visual-prone neurons, text-prone neurons, multimodal-prone neurons, unknown-prone neurons) of InternVL 2.5. We treat the determination of the neuron type as a classification problem.

8 Experiments on another typical VLM of InternVL 2.5 (8B)

In the main manuscript, we performed experiments on top of LLaVA-1.5 (7B) [16]. In this section, we show the analysis and results for another typical VLM of InternVL 2.5 (8B) [9].

8.1 Neuron activation dataset

Similarly to the experiments on LLaVA-1.5, we collected a dataset of neuron activations from the FFN layers on InternVL 2.5. For each neuron, we meticulously select the top $N = 50$ samples that generate the maximum response values from the 23k samples for analysis. Given that InternVL 2.5 8B comprises 32 blocks, with 14,336 neurons in the first linear transformation layer of each FFN layer of a block, there are a total of 458,752 neurons for analysis.

8.2 Distributions of different types of neurons

We estimate the probability of belonging to the four different neuron types by (p_v, p_t, p_m, p_u) . We show the histograms for the probability of p_v , p_t , p_m , and p_u over all the neurons, respectively in Figure 23 (a)-(d).

We can see that only a small fraction of neurons exhibit a high likelihood of belonging to a specific type. Specifically, approximately 8.6% are classified as visual neurons with over an 80% probability; 5.6% exceed this threshold for text neurons; 3.5% for multi-modal neurons; and 12.8% for unknown neurons.

When we consider the identification of neuron type as a classification problem by recognizing the type of high probability as the neuron type, we obtain the class distribution for the four types of neurons for all the (458,752) neurons, as shown in Figure 22. Compared to LLaVA-1.5, InternVL 2.5 exhibits a notable increase in the number of visual-prone neurons and a significant decrease in the proportion of text-prone neurons. This phenomenon may be attributed to the increased emphasis placed by InternVL 2.5 on strengthening its visual data processing capabilities [9], particularly with respect to the handling of multi-image and video input. During

the full model instruction tuning phase (stage 2), the entire model is optimized. In fact, as shown in Figure 23 (a), besides a small portion of neurons that can be clearly identified of their types, there are plenty of neurons that are less confident to be clearly identified as specific neurons.

8.3 Neuron distributions across layers

In this section, we explore the distribution of the four neuron types in the blocks / FFN layers of the model. For each category, we selected top 10,000 neurons ranked by the probability—approximately 2.2% of neurons per type—for our analysis. The distributions of neurons across the layers are shown in Figure 24. For visual neurons and text neurons, they present high frequency in the early and middle layers while low frequency in the high layers. In contrast, the multi-modal neurons have higher frequency in the high layers. That may because in the early and middle layers, more visual neurons and text neurons are learned to focus on processing the individual modality. In the high layers, more multi-modal neurons are learned to jointly deal with visual and text information, enabling efficient reasoning of visual and text information. Interestingly, this distribution trend is similar to that of LLaVA-1.5.

8.4 Explanation quality

We evaluate the quality of generated explanations for different types of neurons, with each explanation generated based on the neuron’s top activated samples. For each neuron type, we randomly selected 800 high-confidence neurons (*i.e.*, neurons whose type classification was unambiguous). As shown in Table 5, the generated explanations are scored of 0.148, 0.194, and 0.185 for visual neurons, text neurons, and multi-modal neurons, respectively.

In addition, we explore the impact of two different sampling strategies for generating explanations: the first method uniformly selects $k = 5$ samples (top 1, 5, 9, 13, 17) from the top 20 samples to elucidate the function of the neuron, while the second randomly chooses five samples from the whole 23k image-text pairs. We conduct simulation of the activations on the uniformly selecting five samples (top 3, 7, 11, 15, 19) from the top 20 samples for each neuron. The more accurate the generated explanations are, the more closely the simulated activations will align with the true neuron activations, resulting in higher evaluation scores. Table 5 shows that the explanations generated from the top samples are more accurate than those of the random samples, indicating the efficiency of the sampling strategy.

Table 5: Explanation quality and impacts of different sampling strategies on three neuron categories for InternVL 2.5.

Neuron category	Top sampling	Random sampling
Visual neurons	0.148	0.132
Text neurons	0.194	0.104
Multi-modal neurons	0.185	0.154

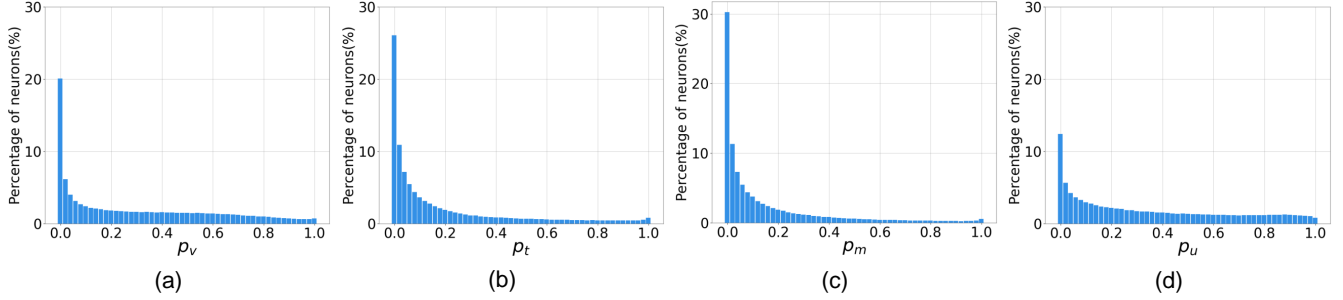


Figure 23: Histogram of InternVL 2.5 for the probability p_v , p_t , p_m , and p_u of belonging to visual neuron, text neuron, multi-modal neuron, and unknown neuron types, respectively.

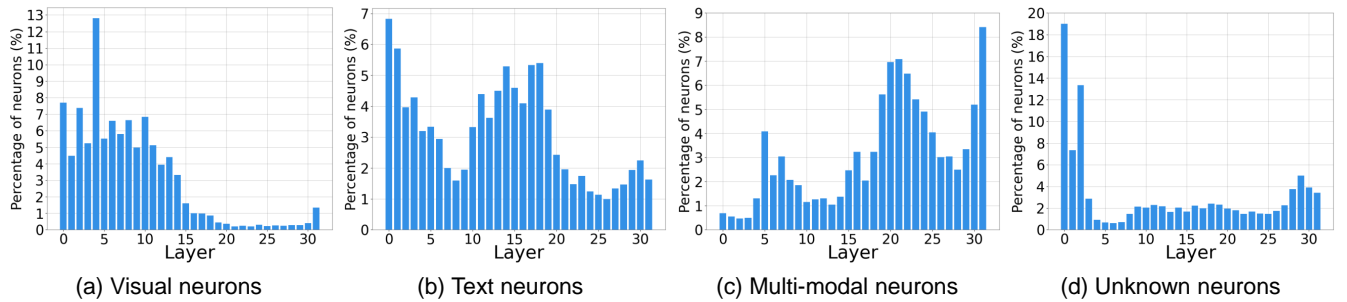


Figure 24: The distribution of special neurons over different layers of InternVL 2.5. (a)-(d) show four categories of neurons, namely visual, text, multi-modal and unknown neurons. The horizontal axis denotes the model layer, from 0 to 31. The vertical axis denotes the number of neurons in the corresponding layer.

9 Experiments on another typical VLM of Qwen2.5-VL (3B)

In this section, we show the analysis and results for another typical VLM of Qwen2.5-VL (3B) [3].

9.1 Neuron activation dataset

Similarly to the experiments on LLaVA-1.5, we collected a dataset of neuron activations from the FFN layers on Qwen2.5-VL. For each neuron, we meticulously select the top $N = 50$ samples that generate the maximum response values from the 23k samples for analysis. Given that Qwen2.5-VL 3B comprises 36 blocks, with 11,008 neurons in the first linear transformation layer of each FFN layer of a block, there are a total of 396,288 neurons for analysis.

9.2 Distributions of different types of neurons

We estimate the probability of belonging to the four different neuron types by (p_v, p_t, p_m, p_u) . We show the histograms for the probability of p_v , p_t , p_m , and p_u over all the neurons, respectively in Figure 25 (a)-(d).

We can see that only a small fraction of neurons exhibit a high likelihood of belonging to a specific type. Specifically, approximately 17.0% are classified as visual neurons with over an 80% probability; 9.6% exceed this threshold for text neurons; 1.5% for multi-modal neurons; and 25.6% for unknown neurons.

When we consider the identification of neuron type as a classification problem by recognizing the type of high probability as

the neuron type, we obtain the class distribution for the four types of neurons for all the (396,288) neurons, as shown in Figure 27. In comparison to LLaVA-1.5, the Qwen2.5-VL exhibits a notable increment in the quantity of visual-prone neurons and a significant decrease in the proportion of text-prone neurons, which is similar to that of InternVL 2.5. This phenomenon may be attributed to the increased emphasis placed by Qwen2.5-VL on enhancing its visual data processing capabilities. In fact, as shown in Figure 25 (a), besides a small portion of neurons that can be clearly identified of their types, there are plenty of neurons that are less confident of being clearly identified as specific neurons.

9.3 Neuron distributions across layers

In this section, we explore the distribution of the four neuron types in the blocks / FFN layers of the model. For each category, we selected top 10,000 neurons ranked by the probability—approximately 2.5% of neurons per type—for our analysis. The distributions of neurons across the layers are shown in Figure 26. For visual neurons, they present high frequency in the early layers, being more concentrated than InternVL 2.5. Particularly, its visual neurons are concentrated in the first two blocks (with ratio 47.6%), unlike LLaVA-1.5 (10.7%) and InternVL 2.5 (12.2%), which show broader distribution. Similar to InternVL 2.5, the multi-modal neurons have higher frequency in the high layers. Interestingly, unlike LLaVA-1.5 and InternVL 2.5, we observe an interleaved distribution of neurons

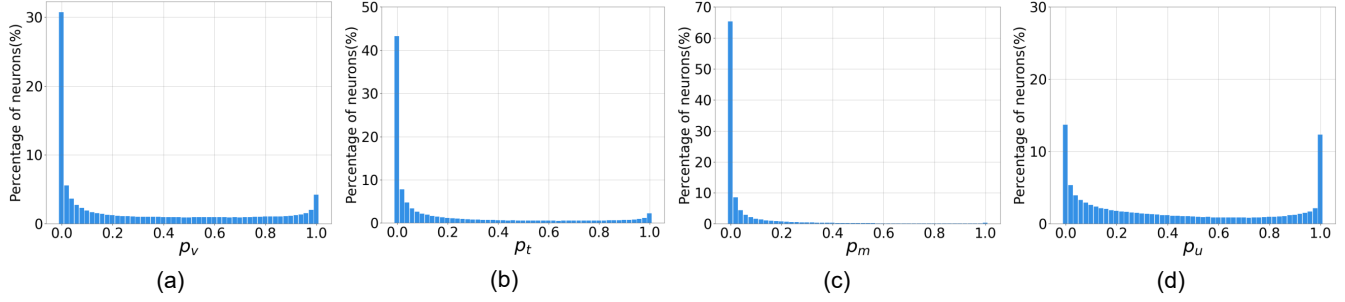


Figure 25: Histogram of Qwen2.5-VL for the probability p_v , p_t , p_m , and p_u of belonging to visual neuron, text neuron, multi-modal neuron, and unknown neuron types, respectively.

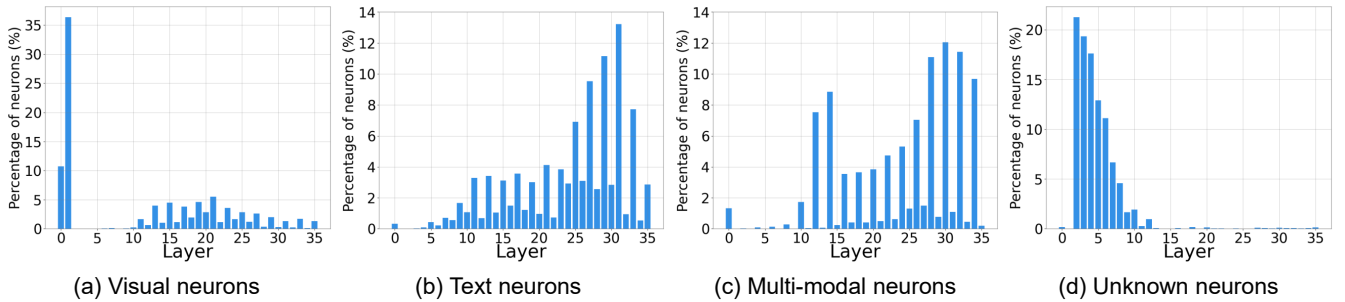


Figure 26: The distribution of special neurons over different layers of Qwen2.5-VL. (a)-(d) show four categories of neurons, namely visual, text, multi-modal and unknown neurons. The horizontal axis denotes the model layer, from 0 to 35. The vertical axis denotes the number of neurons in the corresponding layer.

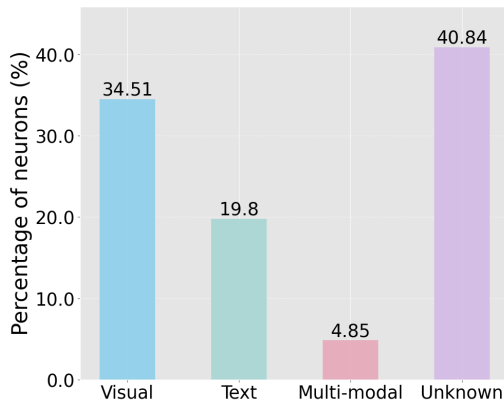


Figure 27: Distribution of the four types of neurons (visual-prone neurons, text-prone neurons, multimodal-prone neurons, unknown-prone neurons) of Qwen2.5-VL. We treat the determination of the neuron type as a classification problem.

across layers. Specifically, visual neurons and text neurons occur significantly more frequently in odd-numbered layers, while their presence drops sharply in even-numbered layers. In contrast, multi-modal neurons appear with greater frequency in even-numbered layers. This pattern suggests that some network blocks may specialize in processing uni-modal information, whereas other blocks are more predisposed to handling multi-modal information.

Table 6: Explanation quality and impacts of different sampling strategies on three neuron categories for Qwen2.5-VL.

Neuron category	Top sampling	Random sampling
Visual neurons	0.152	0.084
Text neurons	0.164	0.106
Multi-modal neurons	0.197	0.111

9.4 Explanation quality

We evaluate the quality of generated explanations for different types of neurons, with each explanation generated based on the neuron's top activated samples. For each neuron type, we randomly selected 800 high-confidence neurons (*i.e.*, neurons whose type classification was unambiguous). As shown in Table 6, the generated explanations are scored of 0.152, 0.164, and 0.197 for visual neurons, text neurons, and multi-modal neurons, respectively.

In addition, we explore the impact of two different sampling strategies for generating explanations: the first method uniformly selects $k = 5$ samples (top 1, 5, 9, 13, 17) from the top 20 samples to elucidate the function of the neuron, while the second randomly chooses five samples from the whole 23k image-text pairs. We conduct simulation of the activations on the uniformly selecting five samples (top 3, 7, 11, 15, 19) from the top 20 samples for each

neuron. The more accurate the generated explanations are, the more closely the simulated activations will align with the true neuron activations, resulting in higher evaluation scores. Table 6 shows that

the explanations generated from the top samples are more accurate than those of the random samples, indicating the efficiency of the sampling strategy.